Heliyon 10 (2024) e29166

Contents lists available at ScienceDirect

Heliyon

journal homepage: www.cell.com/heliyon

Research article

Revealing the active ingredients and mechanism of *P. sibiricumm* in non-small-cell lung cancer based on UPLC-Q-TOF-MS/MS, network pharmacology, and molecular docking

Kaili Guo [a,b,c,1], Yu Jiang [a,b,c,1], Wei Qiao [d,1], Panpan Yuan [a,b,c], Miao Xue [a,b,c], Jiping Liu [a,b], Hao Wei [b], Bin Wang [b], Xingmei Zhu [a,b,c,*]

[a] *Department of Pharmacology, Shaanxi University of Chinese Medicine, Shaanxi, Xianyang, 712046, China*
[b] *Key Laboratory of Pharmacodynamics and Material Basis of Chinese Medicine of Shaanxi Administration of Traditional Chinese Medicine, Shaanxi Xianyang, 712046, China*
[c] *Shaanxi Key Laboratory of Traditional Medicine Foundation and New Drug Research, Shaanxi, Xianyang, 712046, China*
[d] *521 Hospital of NORINCO GROUP, Shaanxi, Xi'an, 710065, China*

ARTICLE INFO

Keywords:
P. sibiricumm
Non-small-cell lung cancer
UPLC-Q-TOF-MS/MS
Network pharmacology
Molecular docking

ABSTRACT

The alcohol extraction of *P. sibiricum* has exhibited significant inhibitory effects on the production of free radicals and the proliferation of non-small-cell lung carcinoma (NSCLC) A549 cells. Despite the diverse components found in alcohol extraction of *P. sibiricum* and its multiple targets, the active components and associated targets remain largely unidentified. Hence, there is a need for additional investigation into the pharmacodynamic elements and mechanisms of action. This study aimed to analyze and identify the components responsible for the anti-tumor activity of alcohol extraction from *P. sibiricum* using UPLC-Q-TOF-MS/MS for the first time. Subsequently, the targets of the active components were predicted using the SwissTargetPrediction database, whereas the targets for NSCLC were sourced from the Online Mendelian Inheritance in Man database (OMIM) and the GeneCards database. Next, the targets of chemical composition were integrated with disease targets via Venny online. GO and KEGG pathway enrichment analyses were performed utilizing DAVID. Subsequently, a network analysis of "components-targets-pathways" was established using Cytoscape 3.8.2 and assessed with the "network analyzer" plug-in. Molecular docking was conducted utilizing Autodock 1.5.6. The study aimed to examine the anti-proliferative impacts and underlying mechanisms of alcohol extraction from *P. sibiricum* on NSCLC through in vivo and in vitro investigations utilizing an animal model of transplanted tumor, CCK8 assay, cell scratch test, RT-qPCR, and western blotting. The study unveiled that 17 active components extracted from *P. sibiricum* alcohol demonstrated anti-non-small cell lung cancer (NSCLC) effects through the modulation of 191 targets and various significant signaling pathways. These pathways include Endocrine resistance, PI3K/AKT, Chemical carcinogenesis-receptor activation, Proteoglycans in cancer, EGFR tyrosine kinase inhibitor resistance, AMPK signaling pathway, and other related signaling pathways. Network analysis and molecular docking results indicated that specific compounds such as (25S)-26-O-(β-D-glucopyranosyl)-

* Corresponding author. Department of Pharmacology, Shaanxi University of Chinese Medicine, Shaanxi, Xianyang, 712046, China.
E-mail addresses: 1204931755@qq.com (K. Guo), 18192024779@163.com (Y. Jiang), popular-2002@163.com (W. Qiao), 1124999618@qq.com (P. Yuan), 3477114970@qq.com (M. Xue), liwenjie780711@163.com (J. Liu), wangbin812@126.com (B. Wang), zhuzhu_sky8169@163.com, zhuzhu_sky8169@163.com (X. Zhu).
[1] These authors contributed equally to this work: Kaili Guo, Yu Jiang and Wei Qiao.

https://doi.org/10.1016/j.heliyon.2024.e29166
Received 19 August 2023; Received in revised form 27 March 2024; Accepted 2 April 2024
Available online 3 April 2024

furost-5-en3β,22α,26-triol3-O-β-D-glucopyranosyl-(1→2)-β-D-glucopyranosyl-(1→4)-β-D-glucopyranoside, Timosaponin H1, Deapi-platycodin D3, (3R)-5,7-dihydroxy-6,8-dimethyl-3-(4′-hydroxybenzyl)-chroman-4-one, Disporopsin, Funkioside F, Kingianoside E, Parisyunnanoside H, and Sibiricoside B primarily targeted 17 key proteins (BCL2, EGFR, ESR1, ESR2, GRB2, IGF1R, JUN, MAP2K1, MAPK14, MAPK8, MDM2, MMP9, mTOR, PIK3CA, RAF1, RPS6KB1, and SRC) collectively. In conclusion, the alcohol extraction of *P. sibiricum* demonstrated inhibitory effects on cell proliferation, induction of apoptosis, and inhibition of metastasis through various pathways.

1. Introduction

Lung cancer remains the primary cause of cancer-related deaths globally, with a consistent rise in morbidity and mortality rates each year. Non-small cell lung cancer (NSCLC) constitutes the majority (85 percent) of lung cancer cases [1]. Standard treatments for NSCLC, including surgical interventions, radiotherapy, systemic chemotherapy, and personalized molecular-targeted therapy, have played a significant role in enhancing the overall survival rates of patients [2,3]. Nevertheless, these therapeutic approaches, whether administered independently or concurrently, frequently entail significant adverse reactions such as gastrointestinal disturbances, bone marrow suppression, hepatotoxicity, and nephrotoxicity, which may adversely affect the quality of life of patients [3–7]. Given the constraints of existing therapeutic methods, recent studies have delved into the potential advantages of incorporating adjuvant chemotherapy with Traditional Chinese Medicine (TCM) to reduce toxicity and improve treatment outcomes for patients with non-small cell lung cancer NSCLC [8–12]. Hence, additional research is necessary to clarify the fundamental mechanisms of action of effective and safe Chinese herbal medicines in the clinical treatment of NSCLC.

The plant species *P. Sibiricum*, belonging to the Liliaceae family, is commonly classified into three varieties: *Polygonatum kingianum Coll.et Hemsl.*, *Polygonatum sibiricum Red.* (*P. sibiricum*) and *Polygonatum cyrtonema Hua*. This study was centered on *Polygonatum sibiricum Red*. sourced from Shaanxi province, the plant is commonly known as chicken head *Polygonatum sibiricum* because of its unique shape that resembles a chicken's head. This plant is distinguished by its petite stature, sweet and adhesive qualities, and is conventionally acknowledged for its dual functionality in medicinal and culinary contexts [13,14]. Chinese traditional medicine has maintained the belief that *P. sibiricum* possesses a peaceful nature, a sweet taste, and has the ability to enter the lung, spleen, and kidney meridians [15]. Hence, it serves the purposes of heart and lung warming, replenishing "qi," enhancing complexion, nourishing the kidneys, fortifying muscles and bones, invigorating essence, promoting mental well-being, supporting the five zang-organs, regulating body temperature, and more. The treatment aims to address conditions such as deficiency of heart and lung qi, spleen and stomach deficiency, kidney and lung dryness, lung and yin deficiency, diabetes resulting from yin deficiency and internal heat, as well as fatigue, among others [16]. Simultaneously, it served as a crucial element in numerous TCM formulations. The pharmacological effects of the substance primarily occur through the regulation of various signaling pathways, including oxidative stress, inflammatory response, fibrosis, lipid metabolism, apoptosis, and others [17–19]. The efficacy of this treatment has been validated in addressing Alzheimer's disease, protecting the heart and kidneys, combating fatty liver, and inhibiting tumor growth, among other benefits [20–25]. *P. sibiricum* plays a crucial role in the treatment regimens prescribed by the distinguished Chinese medicine expert Professor Xu Hefen for NSCLC, focusing on the principles of correction and exorcism. Moreover, it has been noted that this intervention improves the quality of life and sleep patterns in patients with NSCLC, decreases levels of tumor markers, and enhances immunity by strengthening the spleen and kidneys. Existing pharmacological research has primarily concentrated on aqueous extracts and polygonatum polysaccharides, while other components such as saponins, flavonoids, volatile oils, and alkaloids have received limited attention. Previous studies have emphasized the significant anti-free radical and anti-proliferative characteristics of the alcohol extract of *P. sibiricum*, which is enriched with total flavonoids, against A549 cells in an in vitro setting. This research extends the investigation of the alcohol extract of *P. sibiricum* because of its potential as an anti-NSCLC agent, abundant availability, well-established cultivation methods, and widespread distribution in Shaanxi province.

The application of Ultra-Performance Liquid Chromatography-Quadrupole Time-of-Flight Mass Spectrometry (UPLC-Q-TOF-MS/MS) introduces an innovative method for the qualitative and quantitative evaluation of bioactive compounds found in natural products [26,27]. The method is applicable for qualitative, quantitative, and structural analysis of trace components in crude extracts even in the absence of reference material. It offers the benefits of high efficiency, rapid speed, and heightened sensitivity. In this investigation, UPLC-Q-TOF-MS/MS was employed to conduct a qualitative analysis of the alcohol extract derived from *P. sibiricum*. This approach facilitated the determination of precise molecular weights and molecular fragment details. The principal anti-tumor constituents of the alcohol extract of *P. sibiricum* were determined through a comprehensive analysis in conjunction with existing literature. Network pharmacology, conversely, is grounded in systems biology theory and employs a systems perspective and holistic approach to investigate the molecular interactions among drugs, drug combinations, or drug-target interactions [28,29]. Network pharmacology represents a significant advancement in the interdisciplinary integration of information science, medicine, and life science. It serves as a pivotal indicator of the shift from reductionist approaches towards a more systematic exploration in the research of both Chinese and Western medicine. The research concept aligns with the holistic principles of TCM, a tradition that has been passed down for millennia. Additionally, it introduces a novel approach to investigating the complex system of Chinese medicine. The application of Network pharmacology has been extensive in drug discovery and the identification of active compounds in TCM. It plays a crucial role in elucidating the overall mechanism of action, analyzing drug combinations and prescription compatibility, and offering novel scientific and technological advancements to support the rational utilization of TCM and the research and development of new drugs [29–31]. In

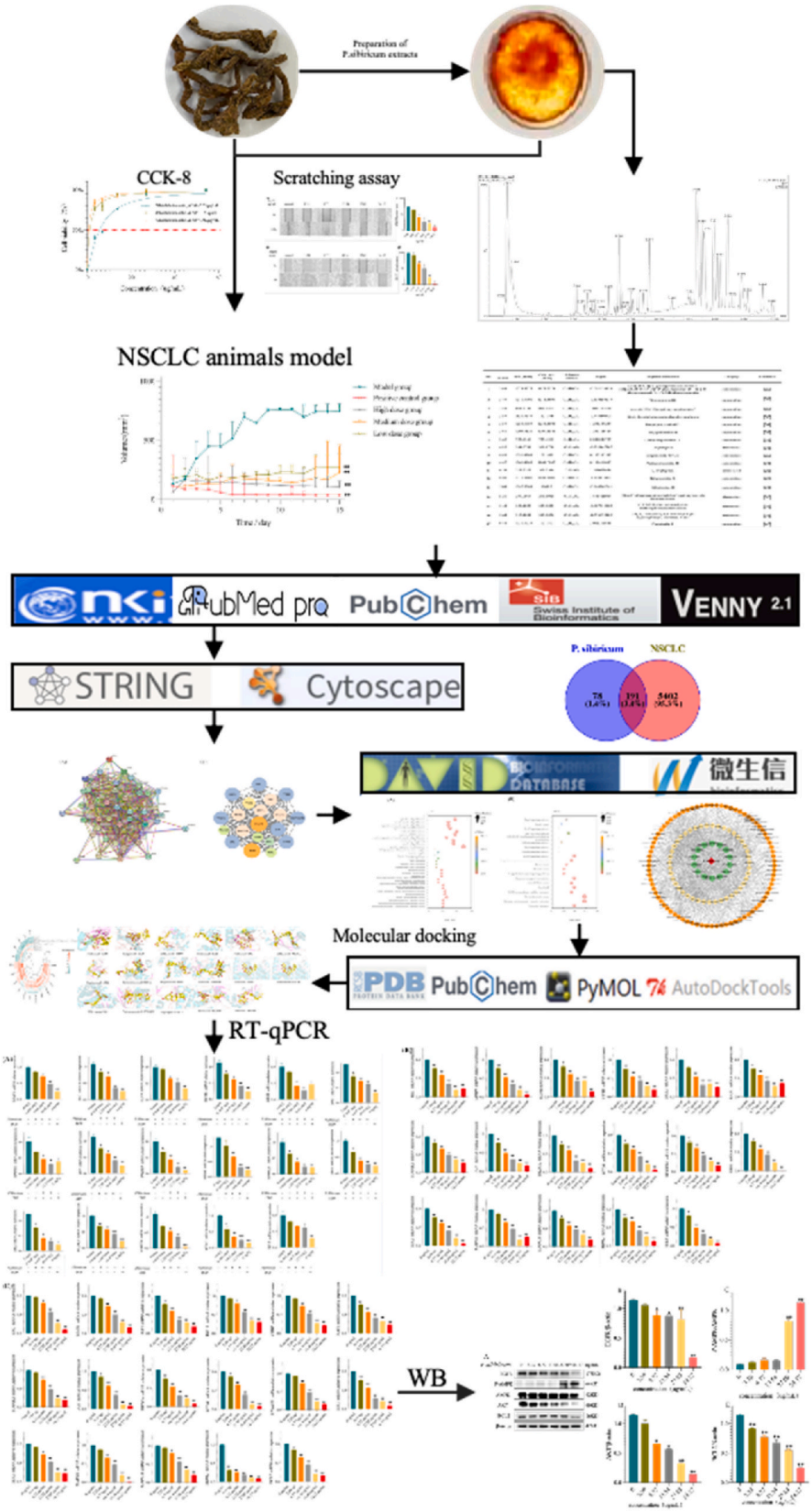

Fig. 1. Technical route diagram of UPLC-Q-TOF-MS/MS combined with network pharmacology to study the action of *P. sibiricum* treating NSCLC.

this specific investigation, the integrated utilization of UPLC-Q-TOF-MS/MS and network pharmacology was utilized to investigate the fundamental components and mechanisms of action of the alcohol extract of *P. sibiricum* (0.512 ± 0.009 mg total flavonoid content equivalent/g dry weight) against NSCLC. The mechanism was further confirmed through RT-qPCR and Western blot analyses. The research methodology utilized in this study is depicted in Fig. 1.

2. Materials

P. sibiricumm (batch No. 202110, Shaanxi Lueyang), which was authenticated by professor Yonggang Yan, School of Pharmacy, the Shaanxi University of Chinese Medicine. DDP (batch No. 15663-27-1, Beijing Puxitang), RPMI-1640 (batch No. PM150110, Procell), DMEM high glucose medium (batch No. PM150210, Procell), FBS (batch No. 900-108, Gemini), penicillin (batch No.A6180, Biotopped), streptomycin (batch No. H18F10Z80985, Shanghai Yuanye), RIPA lysis (batch No. P0013B, Beyotime), BCA Protein Assay kit (batch No. 092721220221, Beyotime), 0.25% Trypsin (batch No. C125C1, HCM Biotech), 0.4% TrypanBlue Staining Solution (batch No. 20210830, Phygene), CCK8 (batch No. EG20220915, EnoGeneCell), SDS-PAGE protein loading buffer (batch No. P0015L, Beyotime), Ultra sensitive ECL chemiluminescence ready to use substrate (batch No. 16J28C97, Boster), marker (batch No. PL00001, Proteintech), Total RNA reagent (Trizol) (batch No. BS259A, Biosharp), 5 × SmArt RT Master Mix (batch No. DY10502, DIYIBio), 2 × RT-qPCR SmArt Mix (batch No. 0650906, DIYIBio).

2.1. In vitro and in vivo test

Cell culture. The Human NSCLC cell lines (A549, NCI–H1299, Procell) and the mouse lung cancer cell line (LLC, Procell) were cultured in DMEM or RPMI-1640 medium which were pre-treated with 10 % fetal bovine serum (FBS), penicillin and streptomycin (100 U/mL, Hyclone, USA). All of them were in a humidified incubator with 5 % CO_2 at 37 °C.

Cell viability assay. NCI–H1299 cells were seeded and cultured into the 96-well microplates at a density of 2×10^3/well in 200 μL DMEM medium for 24 h. Then, the cells were treated with various concentrations of *P. sibiricumm* extracts (0, 3.39, 6.77, 13.54, 27.09, 54.17 μg/mL). After treatment for 24, 48, and 72 h, 10 μL of Cell Counting Kit-8 (CCK8) was added to each well and then cultured for 3.5 h. The absorbance was analyzed at 450 nm using a microplate reader (iMark, Bio-Rad, Hercules, CA, USA). The proliferation of cells was expressed by the absorbance.

Cell scratch test. Cell lines A549, NCI–H1299 were inoculated into the 6-well plates, and cultured in 4.0 mL DMEM with 10 % FBS till to 90 % fusion, with almost no inter-cellular gap, and a single scratch was made using a sterile 200 μL pipette tip. The cells were then incubated with FBS-free culture medium for 24 h to rule out potential effects of FBS on cell migration. Then cells were incubated with culture medium containing different concentrations of *P. sibiricumm* extracts (0, 3.39, 6.77, 13.54, 27.09, 54.17 μg/mL) for another 24 h. Scratches images were taken at 0 and 24 h respectively under an inverted fluorescence microscope (Nikon Eclipse Ti–S, Japan) at 20× magnification. Scratch width was analyzed using ImageJ software. The closure area of the wound was calculated as follows: migration area (%) = $(A_0 - An)/A_0 \times 100$, where A_0 represents the initial area of the wound, and An represents the remaining area of wound at the measurement point.

Animals and Experimental Protocols. Six-week-old C57BL/6 mice (male, ~20 g, SPF) were purchased from Dashuo Technology Co., Ltd. (Chengdu, China). The rearing conditions were temperature 20 ± 2 °C, humidity 60 ± 5 %, 12 h/12 h light-dark cycle, and free access to food and drinking water. After 7 days of feeding, LLC lung cancer cell suspension with a density of 2×10^6 was injected into the right axilla of the animals. About 12 days after inoculation, LLC lung cancer tumor bearing mice with good growth were selected as the tumor source. The skin was removed and the tumor tissue was peeled. The necrotic tissue and normal tissue were removed as far as possible, and the tumor tissue was cut into small pieces with scissors. Finally, the tissue was completely digested with trypsin, and was filtered through a 200-mesh wire mesh to achieve a single-cell suspension. The obtained cell suspension was counted by 0.4 % trypan blue staining to ensure that the number of living cells was greater than 99 %. The concentration of LLC lung cancer cells was adjusted to 1×10^6/mL, and 0.2 mL was subcutaneously injected into the right axillary pit of mice. The blank group received the same dose of PBS. The whole process strictly follows the principle of aseptic operation. After successful molding, the mice were randomly assigned for model control group, positive group (DDP), high-dose group, middle-dose group and low-dose group. At approximately 14 days after modeling, the drug intervention was initiated when the tumor diameter was ≥6 mm measured by vernier scale. The daily dosages of high-dose group, middle-dose group and low-dose group were 18.45 mg/g, 1.845 mg/g, 0.1845 mg/g, respectively. The positive group was given DDP 6 mg/kg once a day. The model group were given the same 0.3 mL saline once a day for 17 days. Tumor volume were measured daily. Tumor volume was calculated using the following formula: Volume (mm^3) = $A \times B^2/2$, where A is the longest diameter (mm) and B is the shortest diameter (mm).

2.2. UPLC-Q-TOF-MS/MS analyses

Preparation of the test solution of P. sibiricumm. P. sibiricumm was dried and crushed, and sieved by No. 6, and 2.00 g of powder was precisely weighed. Then 1.0000 g powder was soaked in 50 % ethanol and ultrasonically extracted for 20 min at 50 °C with the assistance of 0.04 g activated cellulase. The solution was then inactivated in a boiling bath for 10 min. After that, the filtrate was evaporated, and the concentrated liquid was cooled at 4 °C for 4 h, then at −80 °C for 24 h. Finally, the filtrate was placed in a freeze-dryer for 48 h to obtain the lyophilized powder of *P. sibiricum*. The lyophilized powder was dissolved in 50 % methanol to obtain the solution to be tested.

Chromatographic and mass spectrometry conditions. Chromatographic conditions: ACQUITY UPLC HSS T3 C_{18} Column (2.1 mm ×

100 mm, 1.8 μm); mobile phase: 0.1 % formic acid water (A) and acetonitrile (B), gradient elution: (0–2 min, 90 %-75 % A; 2–3 min, 75 %–65 % A; 3–4 min, 65 %–50 % A; 4–5.5 min, 50 %–45 % A; 5.5–7.5 min, 50 %–45 % A; 7.5–10 min, 45 %–35 % A); column temperature: 35 °C; flow rate: 0.4 mL/min; injection volume: 2.0 μL. Mass spectrum conditions: ion source (ESI source); scanning mode (negative ion scanning); scanning range (*m/z*, 100–1500); desolvation temperature: 400 °C; desolvation gas flow rate: 800L/h; LockSpray: [5-Leucine]Enkephalin(LE); Data acquisition software: MassLynx 4.1.

Identification of compounds. The relative molecular mass of the compound was estimated according to the molecular ion peaks provided by multi-stage mass spectrometry and high-resolution mass spectrometry, and the relative molecular mass was calculated according to the molecular formula of each component by the Molecular Weight Calculator tool of Masslynx v4.1 software. Use CNKI, ScienceDirect, Web of Science, TCMSP and other domestic and foreign databases to collect various chemical components and names of *P. sibiricumm* plants. Then, according to the retention time given by UPLC-Q-TOF-MS/MS and the mass spectrometry fragment information provided by the SciFinder database, the accurate identification of the compounds was finally achieved by comparing the relevant literature.

2.3. Network pharmacology research and validation

Collection and integration of active components of P. sibiricumm and disease targets. Firstly, the canonical SMILES of each identified active compounds of *P. sibiricumm* was achieved through the PubChem (https://pubchem.ncbi.nlm.nih.gov/), then those SMILES got were imported into the SwissTargetPrediction online server (http://www.swisstargetprediction.ch/). The species "Homo sapiens" and the probability >0 was selected as the screening condition, and the duplicate targets were deleted. Secondly, the NSCLC targets were obtained by searching GeneCards (GeneCards, https://www.genecards.org/) and the Online Mendelian Inheritance in Man (OMIM, https://omim.org/) databases using the keyword "Non-small cell lung cancer" or "NSCLC". Finally, the intersection targets of *P. sibiricumm* and NSCLC was integrated through Venny 2.1 (https://bioinfogp.cnb.csic.es/tools/venny/index.html) as the possible targets against NSCLC.

Gene ontology(GO) annotation and kyoto encyclopedia of genes and genomes (KEGG) enrichment analysis. The integrated targets of P. sibiricumm and NSCLC were entered into DAVID database (https://david.ncifcrf.gov), and then defined "official gene symbol" as select identifier,set species as "Homo Sapiens" for GO and KEGG enrichment analysis, and the enrichment results were presented with online wechat platform (http://www.bioinformatics.com.cn) as bubble plot.

Construction of the Targets Protein-Protein Interaction (PPI) network. The targets of *P. sibiricumm* for the treatment of NSCLC were imported into the STRING database (https://string-db.org/), and species was set as "Homo Sapiens", the protein interaction relationship was analyzed. The pharmacological network of "active component of *P. sibiricumm*-targets-pathways" was constructed and visualized by Cytoscape 3.8.2. Network Analyzer was used to screen the anti-NSCLC core components (degree ≥5 in the Network) and hub genes.

Molecular docking. The 3D structure of core components of *P. sibiricumm* and hub targets of anti-NSCLC were retrieved from the PubChem database and RCSB PDB database (https://www.pdbus.org), respectively. Then the proteins and compounds were processed by Autodocktool 1.5.6 software and converted into RCSB PDBQT format. Finally, the docking results were visualized using PyMol and Discovery studio Client. The conformations chosen were those with the smallest binding free energy.

Real-time quantitative PCR (RT-qPCR). Total RNA was extracted from tumor-bearing mice and NSCLC cell lines using Trizol reagent according to the manufacturer's instructions. First-strand cDNAs were prepared according to the instructions included with the 5 × SmArt RT Master Mix. Polymerase chain re-actions were performed using specific forward and reverse primers. RT-qPCR was performed using 2 × RT-qPCR SmArt. The relative expression levels of the BCL2, EGFR, ESR1, ESR2, GRB2, IGF1R, JUN, MAP2K1, MAPK14, MAPK8, MDM2, MMP9, mTOR, PIK3CA, RAF1, RPS6KB1 and SRC gene were normalized against β-actin and analyzed via

Table 1
Primers used for quantitative real-time polymerase chain reaction (RT-qPCR) assay.

No.	Gene name	Length	Forward	Reverse
1	EGFR	102	CCTGGAAGAGACCTGCATTATC	GTTAAACCCACTACTGAGACAGG
2	BCL2	133	AGAGCGTCAACAGGGAGAT	GGGCCATATAGTTCCACAAAGG
3	ESR1	119	CCTGGACAGGAATCAAGGTAAA	TGAGGCACACAAACTCTTCTC
4	ESR2	105	GAAGGCCATGATTCTCCTCAA	TCTGTCACTGCGTTCAATAGG
5	GRB2	130	GTCCAGGAACCAGCAGATATTC	AATGAAGTCTCCTCTGCGAAAG
6	IGF1R	99	GGTCCTTTGGGATGGTCTATG	TACTTGCAGCCTCGTTTACC
7	JUN	124	AATGGGCACATCACCACTAC	TGTTCTGGCTATGCAGTTCAG
8	MAP2K1	129	CTTCGGGAGAAGCACAAGATTA	GGAGTTGGCCATAGAGTCAATTA
9	MAPK8	118	GATCCCGGACAAGCAGTTAG	CTGCCCTCTTATGACTCCATTC
10	MAPK14	108	ATGCCTACTTTGCTCAGTACC	TCAGGCTCTTCCACTCATCTA
11	MDM2	148	AACTGGCTTCCAGACGATAAG	CCTCAGCACATGGCTCTTTA
12	MMP9	116	CAATCCTTGCAATGTGGATGTT	CCTGTAATGGGCTTCCTCTATG
13	mTOR	125	ACTGCTTTGAGGTCGCTATG	GTGGCATGTGGTTCTGTAGT
14	PIK3CA	112	CAGAGGTTTGGCCTGCTATT	GGATGTCCGTTAGGTTGATGAG
15	RAF1	121	AATAGAAGCCAGTGAGGTGATG	AGTTGGGTCAACCACCTTTAG
16	RPS6KB1	124	TCAGCCCAGTCAAATTCTCTC	GTCACATCCATCTGCTCTATCC
17	SRC	125	CGGCTCATAGAAGACAACGAATA	ATCCCAAAGGACCACACATC

the 2-ΔΔCt method as described previously. [ΔΔCt = (Ct Target - Ct Reference) sample - (Ct Target - Ct Reference) control]. The primer sequences used in this study are listed in Table 1.

Western blot analysis. NCI–H1299 cells were seeded into 6-well plates at a density of 2×10^5/well, and were treated with various concentrations of *P. sibiricumm* extracts (0, 3.39, 6.77, 13.54, 27.09, 54.17 μg/mL) for 24 h. Next, adding the RIPA lysis buffer (Beyotime) with protease inhibitor on ice. Then, the total protein content was determined by BCA protein Assay kit. The qualified protein sample was adjusted to the same densities and denatured at 100 °C for 5 min. Then they were sequentially separated by SDS-PAGE gel electrophoresis and transferred to PVDF membrane. The transformed membrane was sealed with 5 % BSA at room temperature for 1 h and incubated with the corresponding primary antibody anti-EGFR (BST17124009, 1:1000, BOSTER), anti-p-AMPK (AP0116, 1:1000, Abclonal), anti-AMPK (A7339, 1:1000, Abclonal), anti-AKT (BST17514390, 1:1000, BOSTER), anti-BCL2 (BST17174985, 1:1000, BOSTER), and anti-β-actin (XA5171BP11766, 1:1000, BOSTER) overnight at 4 °C. After rinsed by TBST three times, horseradish peroxidase-labled goat anti-rabbit IgG (1:7500; BOSTER) was added into, and incubated at room temperature for another 1 h. Finally, the ECL developer solution was added and exposed to gel Imager (Syngene, England). Meantime, taking β-actin as the reference protein, Image J 1.53 was used to calculate the gray level of each target protein to obtain its corresponding relative protein level. At least three independent experiments were repeated for each target protein.

Statistical analysis. All data were analyzed using SPSS 26.0. A two-sample *t*-test or one-way analysis of variance was used to analyze continuous variables across groups. All statistical tests were two-tailed, and a value of $P < 0.05$ was considered to indicate statistically significant results.

3. Results

Effects of P. sibiricum in C57/BL6 mice bearing LLC tumors. C57/BL6 mice were implanted with LLC tumor cells, the LLC tumor volume in mice with tumors reached 0.43 cm^3 on the 7th day post-implantation and progressively increased to 1.31 cm^3 by the 15th day. In comparison to the model group, tumor growth was markedly suppressed in mice treated with DDP or different doses of *P. sibiricum* in C57/BL6 mice implanted with LLC cells ($P < 0.01$, Fig. 2).

Effects of P. sibiricum on cell viability in H1299 cells. The H1299 cell line was exposed to varying concentrations of *P. sibiricum* (0, 3.39, 6.77, 13.54, 27.09, 54.17 μg/mL), and cell viability was assessed using the CCK8 assay at 24 h, 48 h, and 72 h time points. The calculated IC50 values were 5.53, 1.12, and 0.56 μg/mL, respectively. The results depicted in Fig. 3 indicate a notable suppression of cell proliferation in the *P. sibiricum*-treated groups compared to the control group, with effects exhibiting a dose-dependent relationship. Furthermore, the inhibitory impact of *P. sibiricum* notably escalated after 48 h. Previous investigations from our research group revealed that the IC50 values of *P. sibiricum* on A549 cells were 25.18, 12.52, and 9.25 μg/mL at 24 h, 48 h, and 72 h, respectively.

Effects of P. sibiricum on cell migration in A549 and H1299 cells. The impact of *P. sibiricum* on cell migration in A549 and H1299 cells was investigated in this study. A549 and H1299 cells were exposed to varying concentrations of *P. sibiricum* (0, 3.39, 6.77, 13.54, 27.09, 54.17 μg/mL), and their migratory behavior was assessed using a scratch wound assay after 24 h (Fig. 4A and B). The results depicted in Fig. 4C and D indicate a significant reduction in cell migration in the groups treated with *P. sibiricum* compared to the control group ($P < 0.01$, $P < 0.05$).

Identification of the chemical components of P. sibiricumm detected by UPLC-Q-TOF-MS/MS. The samples were subjected to analysis utilizing the liquid chromatography and mass spectrometry parameters outlined previously. In the negative ion detection mode of electrospray ionization (ESI), distinct fragmentations of flavonoid aglycones were observed (Fig. 5). These specific ions serve as valuable indicators for the identification of flavonoids. Through the utilization of online databases, consultation of pertinent literature, and adherence to compound fragmentation principles, a qualitative assessment of the *P. sibiricum*-related compounds was conducted. A total of thirty-one compounds were successfully characterized, encompassing acids, sugars, glycosides, esters, and flavonoids. The total ion chromatogram of *P. sibiricum* is depicted in Fig. 5, while Table 1 presents the retention times, *m/z* values, molecular formulas, and the identified compounds (Table 2).

Network pharmacology analysis. To screen the target of chemical constituents of P. sibiricum for treatment of NSCLC. A comprehensive

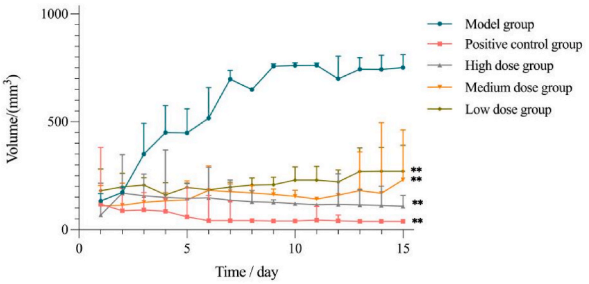

Fig. 2. *P. sibiricum* had anti-NSCLC effect. C57/BL6 mice bearing LLC tumors were randomly assigned to the model, positive control, high dose of *P. sibiricum*, medium dose of *P. sibiricum*, and low dose of *P. sibiricum* groups (n = 6, each group). The line graph represents tumor volume from five different animals, data are expressed as the Mean ± SD. The tumor growth was significantly inhibited in various *P. sibiricum* groups. $^{**}P < 0.01$ as compared with Model group. LLC: Lewis lung cancer.

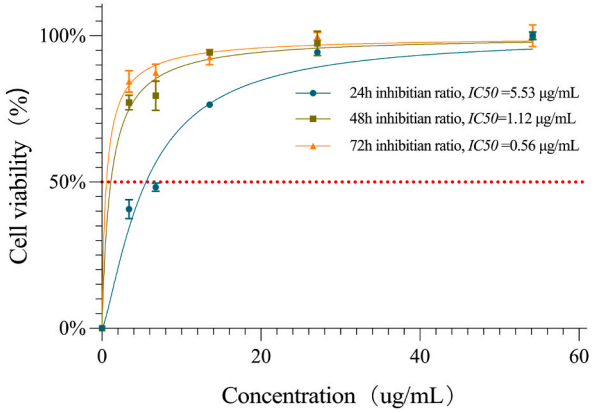

Fig. 3. Analysis of H1299 cells proliferation in different treatment groups. n = 4 per group.

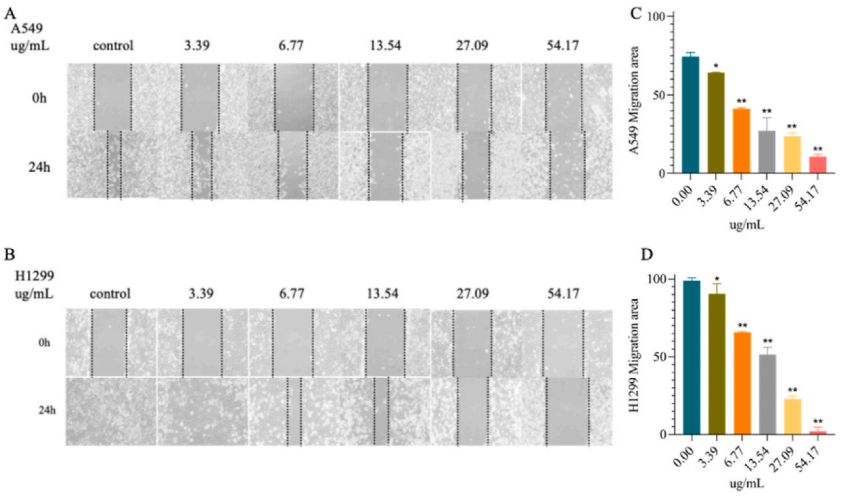

Fig. 4. Effects of *P. sibiricum* on the migration of NSCLC cells tested by the scratch wound assay. (A)The migration of A549 cells in different treatment groups. (B)The migration of H1299 cells in different treatment groups. (C) Quantitative analysis of the migration rates in A. (D) Quantitative analysis of the migration rates in B. Data are presented as the Mean ± SD (n = 3). *$P < 0.05$; **$P < 0.01$ as compared with 0.00 μg/mL.

analysis was conducted to predict targets associated with *P. sibiricum* using the Swiss Target Prediction method, resulting in the identification of 269 potential targets. Furthermore, a total of 5593 genes related to NSCLC were extracted from GeneCards and OMIM databases. Subsequently, an intersection analysis was performed using Venny software, revealing 191 common targets among the identified genes (Fig. 6).

Construction and Analysis of the Target PPI Network. The cross-targets were inputted into Cytoscape software for the purpose of identifying a total of 43 targets with degree values equal to or greater than 36 (Table 3). Through the protein-protein interaction (PPI) network analysis, potential associations among the targets were elucidated. Following the elimination of redundant genes, the resulting PPI network consisted of 43 nodes and 589 edges, exhibiting an average local clustering coefficient of 0.805 (Fig. 7A). For enhanced visualization, a secondary network was constructed to emphasize the top 20 genes among all nodes (Fig. 7B). Node size and color were indicative of the degree of importance, with larger degrees signifying greater significance within the network, potentially designating them as key targets for *P. sibiricum* in the treatment of NSCLC. This analysis effectively unveiled the intricate multi-component and multi-target mechanism underlying the therapeutic effects of *P. sibiricum* alcohol extracts in NSCLC treatment.

GO analysis and KEGG pathway analysis. To elucidate the molecular mechanism involved in the treatment of NSCLC by *P. sibiricum*, an analysis of GO and KEGG pathways was conducted on 191 anticancer targets. The GO analysis revealed 1971 biological processes (BP), 61 cellular components (CC), and 154 molecular functions (MF) (Fig. 8A). In BP regulation, the targets primarily encompass positive regulation of cell migration, muscle cell proliferation, protein kinase B signaling, positive regulation of smooth muscle cell proliferation, myeloid cell differentiation, leukocyte differentiation, myeloid leukocyte differentiation, regulation of smooth muscle cell proliferation, smooth muscle cell proliferation, epithelial cell proliferation, and other related processes. In CC, the targets primarily encompass membrane microdomains, the mitochondrial outer membrane, organelle outer membranes, receptor complexes, RNA polymerase II transcription factor complexes, nuclear transcription factor complexes, ficolin-1-rich granules,

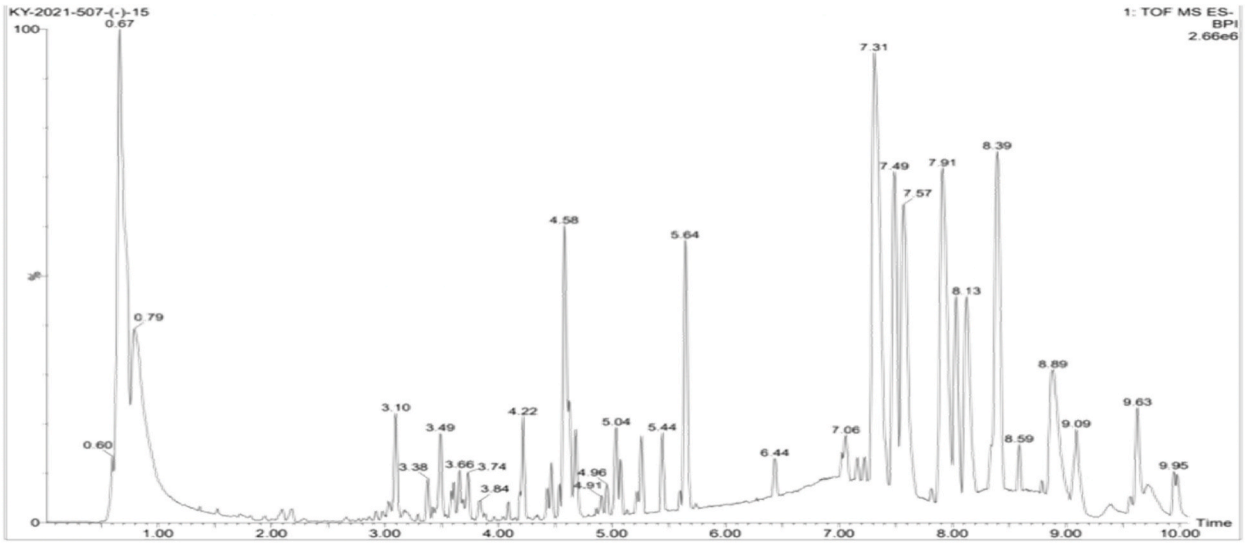

Fig. 5. UPLC-Q-TOF-MS/MS total ion chromatograms of *P. sibiricumm*.

Table 2
Identification of chemical compositions in *P. sibiricumm* by UPLC-QTOF-MS/MS.

No.	tR/ min	*m/z* [M − H]⁻	Calc. m/z [M − H]⁻	Molecular formula	δ/ppm	Proposed compound	Category	Reference
1	3.49	1079.5275	1079.5274	$C_{51}H_{84}O_{24}$	−0.092633128	(25S)-26-O-(β-D-glucopyranosyl)-furost-5-en3β,22α,26-triol3-O-β-D-glucopyranosyl-(1 → 2)-β-D-glucopyranosyl-(1 → 4)-β-D-glucopyranoside	saponosides	[32]
2	3.49	1211.5701	1211.5697	$C_{56}H_{92}O_{28}$	−0.330150217	Timosaponin H1	saponosides	[32]
3	3.59	975.4781	975.4801	$C_{47}H_{76}O_{21}$	2.050272476	Acetyl-(25S,22ξ)-hydroxylwattinoside C	saponosides	[32]
4	3.59	1121.5375	1121.558	$C_{53}H_{86}O_{25}$	0.44580842	didehydro-diol-diosgenin-rha-glc-rha-glc-glc	saponosides	[33]
5	3.59	1253.5787	1253.5803	$C_{58}H_{94}O_{29}$	1.276344244	Deapi-platycodin D3	saponosides	[34]
6	3.66	1209.5526	1209.5541	$C_{56}H_{90}O_{28}$	1.240126424	Polygodoraside B	saponosides	[32]
7	3.69	929.4366	929.4385	$C_{45}H_{70}O_{20}$	2.044244993	(25R)-kingianoside G	saponosides	[32]
8	4.22	301.0709	301.0708	$C_{16}H_{14}O_6$	−0.332147787	Disporopsin	flavonoids	[35]
9	4.43	1091.4908	1091.491	$C_{51}H_{80}O_{25}$	0.183235592	kingianoside G + Glc	saponosides	[32]
10	4.47	1061.4803	1061.4805	$C_{50}H_{78}O_{24}$	0.188416085	Parisyunnanoside H	saponosides	[33]
11	4.58	329.2329	329.2334	$C_{18}H_{34}O_5$	1.518679454	L-tryptophan	amino acid	[36]
12	4.96	1077.5107	1093.5067	$C_{51}H_{82}O_{25}$	1.18883588	Kingianoside E	saponosides	[37]
13	5.04	1047.5009	1063.5	$C_{50}H_{80}O_{24}$	−0.846262341	Sibiricoside B	saponosides	[38]
14	5.26	299.0914	299.0919	$C_{17}H_{16}O_5$	1.671726984	(3R)-5,7-dihydroxy-6-methyl-3-(4′-hydroxybenzyl)-chroman-4-one	flavonoids	[35]
15	5.44	329.1027	329.1025	$C_{18}H_{18}O_6$	−0.607713402	4′,5,7-Trihydroxy-6-methyl-8-methoxylhomoisoflavanones	flavonoids	[39]
16	5.64	313.1081	313.1076	$C_{18}H_{18}O_5$	−1.596895125	(3R)-5,7-dihydroxy-6,8-dimethyl-3-(4′-hydroxybenzyl)-chroman-4-one	flavonoids	[35]
17	6.44	1031.5039	1031.507	$C_{50}H_{80}O_{22}$	3.005311646	Funkioside F	saponosides	[40]

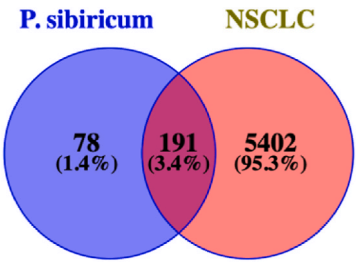

Fig. 6. Venn diagram of *P. sibiricumm*-NSCLC targets.

Table 3
Core targets of PPI network.

No.	Symol	degree	No.	Symol	degree	No.	Symol	degree
1	TNF	115	17	MAPK14	58	33	PRKCA	40
2	EGFR	105	18	FGF2	57	34	RPS6KB1	40
3	SRC	99	19	PIK3CA	57	35	IGF1R	39
4	VEGFA	97	20	STAT1	54	36	KIT	39
5	CASP3	96	21	AR	53	37	HSP90AB1	39
6	ESR1	96	22	GRB2	53	38	CDK1	39
7	JUN	90	23	IL2	51	39	RAF1	38
8	STAT3	85	24	PPARA	50	40	PARP1	38
9	PPARG	84	25	PTPRC	48	41	TERT	38
10	HSP90AA1	80	26	MAPK8	47	42	MET	37
11	PTGS2	78	27	KDR	46	43	ESR2	36
12	mTOR	72	28	CASP8	46			
13	MMP9	69	29	MAPK15	43			
14	BCL2	64	30	FGF3	42			
15	SIRT1	63	31	STAT2	42			
16	MDM2	59	32	MAP2K1	41			

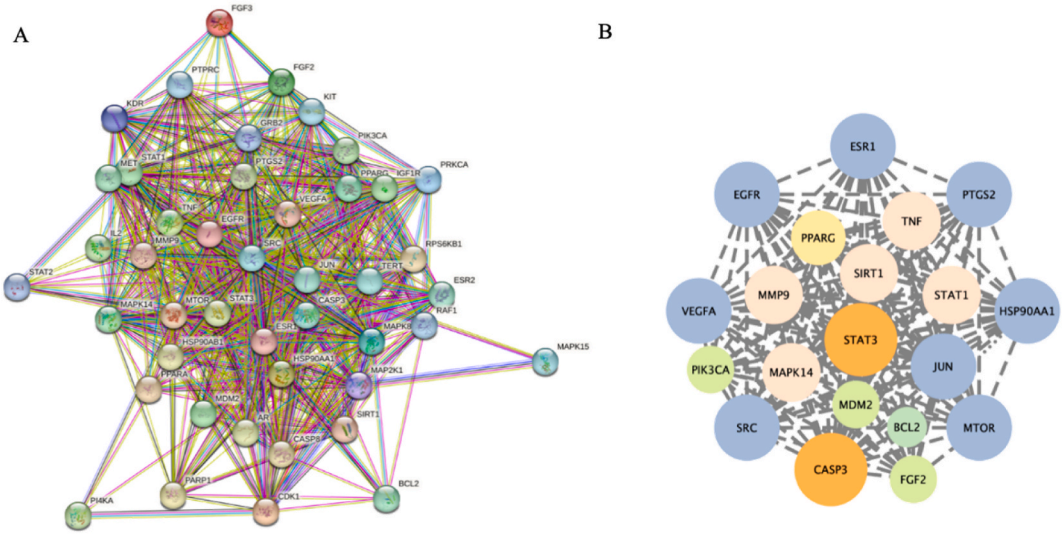

Fig. 7. (A) PPI network of the common target genes; (B) top 20 genes.

phosphatidylinositol 3-kinase complexes, transcription factor complexes, nuclear chromosomes, telomeric regions, and others. In the context of MF, the identified targets primarily encompass phosphatidylinositol bisphosphate kinase activity, protein tyrosine kinase activity, phosphatase binding, signal transducer activity downstream of receptor, protein phosphatase binding, signal transducer downstream of receptor with serine/threonine kinase activity, nuclear receptor activity, transcription factor activity, direct ligand-regulated sequence-specific DNA binding, mitogen-activated protein kinase kinase binding, MAP kinase kinase kinase activity, nuclear hormone receptor binding, hormone receptor binding, among others. A total of 144 pathways were delineated through KEGG pathway analysis, revealing a close association of the targets with pathways such as Endocrine resistance, Chemical carcinogenesis-receptor activation, Proteoglycans in cancer, EGFR tyrosine kinase inhibitor resistance, AMPK signaling pathway, Hepatitis B, MicroRNAs in cancer, Human cytomegalovirus infection, MAPK signaling pathway, Prolactin signaling pathway, and others. The findings indicate that *P. sibiricum* potentially contributes to the management of NSCLC through multiple pathways. Specifically, the endocrine resistance pathway involves 17 potential targets, encompassing a majority of the core genes, and is likely a pivotal pathway. The visualization in Fig. 8 displays the top 20 results of the enrichment analysis. The markedly enriched pathways indicate that the core targets demonstrate a robust correlation with the “endocrine resistance signaling pathway” (Fig. 8B). Through the functional analysis of each target within this pathway, the study identified 17 core targets (Bcl-2, EGFR, ESR1, ESR2, GRB2, IGF1R, JUN, MAP2K1, MAPK14, MAPK8, MDM2, MMP9, mTOR, PIK3CA, RAF1, RPS6KB1, and SRC) with higher degree values. These targets were found to have a closer correlation with the occurrence and progression of tumors, establishing them as the key targets of P. sibiricumm in its anti-NSCLC effects. The aforementioned findings suggest that the primary chemical constituents of *P. sibiricum* were varied and spread across various biological processes, cellular components, and molecular functions, indicating its multi-pathway attributes.

Compound-target-pathway network analysis. A network comprising compounds, targets, and pathways was established utilizing

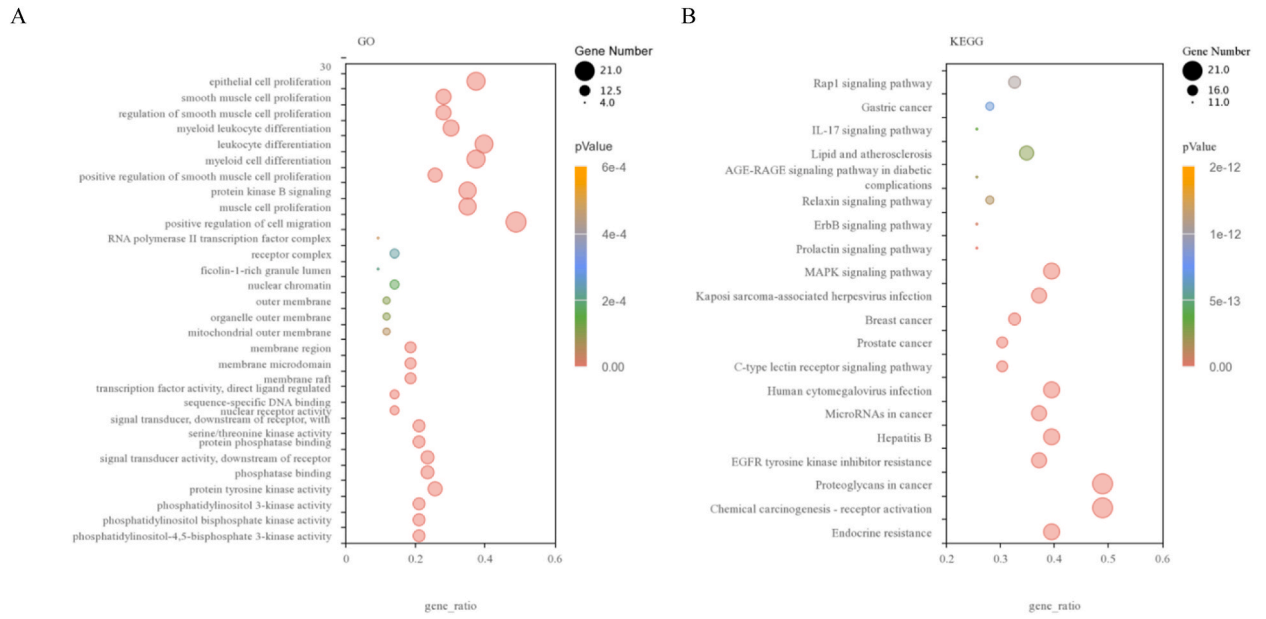

Fig. 8. GO function and KEGG signaling pathway analysis of the core targets of P. sibiricumm. (A) GO function analysis of the core targets genes. (B) KEGG enrichment analysis of the core targets.

Cytoscape 3.8.2 (Fig. 9). The network comprised 14 representative components, 43 representative targets, and 80 representative pathways. From the diagram, it is evident that the targets of *P. sibiricum* active components are distributed across various pathways, coordinating with each other, and collectively contributing to the treatment of NSCLC. This observation comprehensively demonstrates the multi-component, multi-target, and multi-pathway characteristics of TCM.

Molecular docking results. Molecular docking was conducted individually for the 17 compounds identified in *P. sibiricum* (Table 2) with the 17 core targets. The primary constituents of the *P. sibiricum* rhizome extract were identified through an analysis of their binding energy. To assess the binding affinity between essential compounds and specific targets, we employed the empirical threshold of −5.0 kcal/mol, as stipulated in the literature, as the criterion for evaluation [41]. Typically, the compound acts as a ligand, while the target serves as a receptor. If the docking binding energy fell below the specified threshold, it indicated a higher binding affinity between the target and the compound. The docking results revealed that only nine active components listed in Table 2 exhibited strong binding affinity towards the 17 targets. The interactions between these compounds and targets are visually represented in Fig. 10A and 10B. Based on the binding energies presented in Table 4, nine compounds, specifically (25S)-26-O-(β-D-glucopyranosyl)-furost-5-en3β, 22α,26-triol 3-O-β-D-glucopyranosyl-(1→2)-β-D-glucopyranosyl-(1→4)-β-D-glucopyranoside, Timosaponin H1, Deapi-platycodin D3, (3R)-5,7-dihydroxy-6,8-dimethyl-3-(4′-hydroxybenzyl)-chroman-4-one, Disporopsin, Funkioside F, Kingianoside E, Parisyunnanoside H, and Sibiricoside B, were identified as crucial constituents of *P. sibiricum* with potential anti-non-small cell lung cancer (NSCLC) properties. The compounds were subjected to molecular docking with 17 core targets, namely Bcl-2, EGFR, ESR1, ESR2, GRB2, IGF1R, JUN, MAP2K1, MAPK14, MAPK8, MDM2, MMP9, mTOR, PIK3CA, RAF1, RPS6KB1, and SRC, using a lower threshold (≤-5.1 kcal/-mol). These results were consistent with the findings of the KEGG pathway.

P. sibiricum might inhibited NSCLC through down-regulating endocrine resistance. The KEGG pathway analysis identified that the 17 core targets related to *P. sibiricum* were primarily associated with pathways involved in tumor-associated endocrine resistance. Recent studies have confirmed a robust association between endocrine resistance and the onset and advancement of tumors. To confirm the precision of the forecasted targets recognized through network pharmacology analysis, the mRNA expression levels of the 17 key targets, specifically BCL2, EGFR, ESR1, ESR2, GRB2, IGF1R, JUN, MAP2K1, MAPK14, MAPK8, MDM2, MMP9, mTOR, PIK3CA, RAF1, RPS6KB1, and SRC, were evaluated in tumor-bearing mice and NSCLC cell lines using RT-qPCR (Fig. 11A, 11B, and 11C). A comparative analysis of mRNA expression levels between the model or control group and the experimental groups indicated a notable down-regulation of 17 genes, in both tumor-bearing mice and NSCLC cell lines treated with *P. sibiricum*. The findings indicate that *P. sibiricum* might exert inhibitory NSCLC by suppressing endocrine resistance mechanisms.

P. sibiricum might inhibited H1299 through PI3K/AKT passways and EGFR in NSCLC. To validate the mechanism underlying *P. sibiricum* in the treatment of NSCLC, the NCI–H1299 cells were subjected to different dose treatments with *P. sibiricum* for 24 h. Analysis utilizing GO and KEGG pathways revealed a significant association between the pharmacological impacts of *P. sibiricum* and resistance to endocrine therapies, as well as epidermal growth factor receptor (EGFR) resistance, AMP-activated protein kinase (AMPK), and cellular proliferation. Consequently, NSCLC cell line H1299, which is recognized for its resistance to EGFR tyrosine kinase inhibitors (TKI), was selected for additional examination of the effects of *P. sibiricum* on the expression of EGFR, AMPK, AKT, and BCL proteins (Fig. 12A). Despite demonstrating resistance to EGFR TKI, NCI–H1299 cells were observed to have their EGFR kinase activity inhibited upon treatment with *P. sibiricum* (Fig. 12B). Moreover, a decrease in AKT activity was noted in H1299 cells after

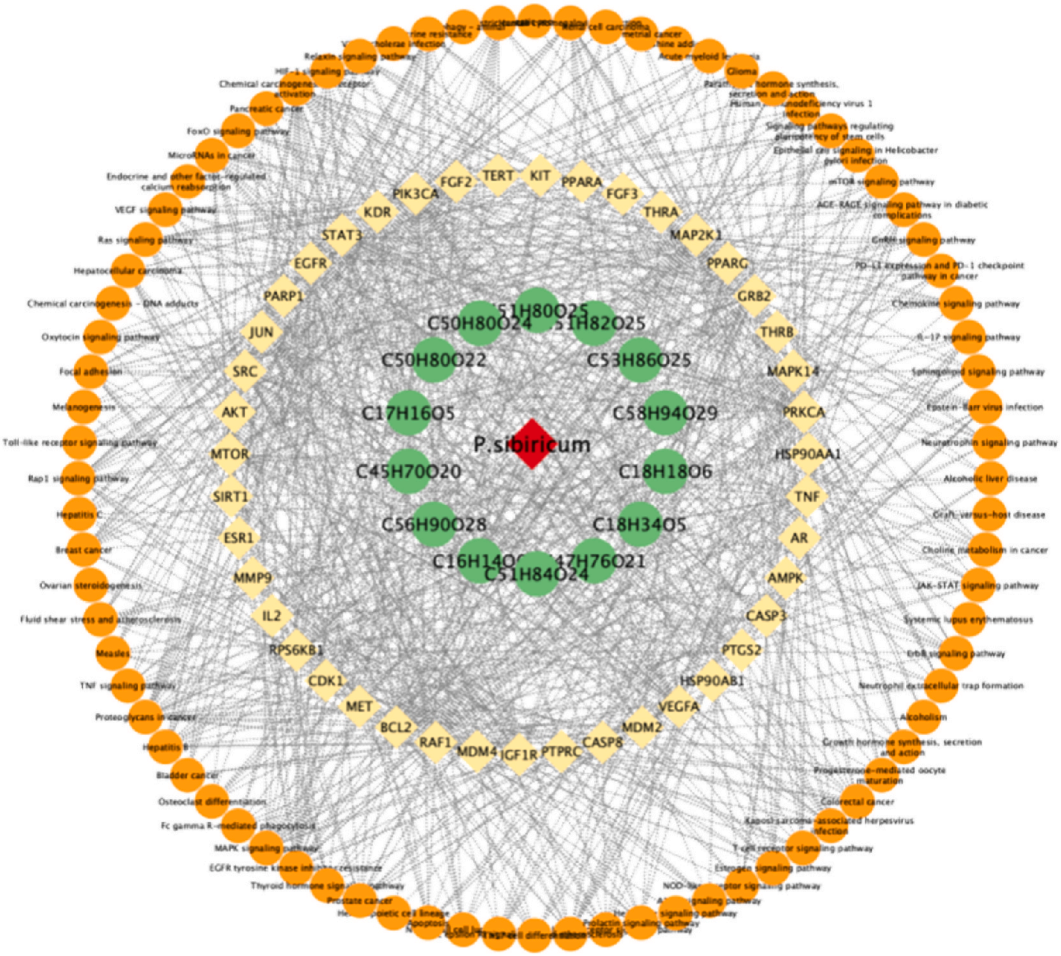

Fig. 9. Compound-target-pathway network. Green circle nodes represent chemical compounds, yellow quadrilateral nodes represent targets, and orange circle nodes represent pathways. (For interpretation of the references to color in this figure legend, the reader is referred to the Web version of this article.)

exposure to *P. sibiricum* (Fig. 12D). Moreover, *P. sibiricum* has been demonstrated to stimulate AMP-activated protein kinase (Fig. 12C) while reducing the levels of BCL2 (Fig. 12E). The findings indicate that *P. sibiricum* has the potential to inhibit the growth of NSCLC cells, promote apoptosis, and exhibit efficacy against cells that exhibit resistance to epidermal growth factor receptor tyrosine kinase inhibitors (EGFR TKI). The results presented in this study are consistent with the hypotheses generated by network pharmacology, thus supporting additional investigations into the anti-NSCLC mechanism of *P. sibiricum*.

4. Discussion

The desiccated rhizome of *Polygonatum* has historically been employed for its diverse medicinal attributes, including anti-aging, antioxidant, bactericidal, anti-herpes, and analgesic properties. The main chemical components identified in *P. sibiricum* consist of polysaccharides, steroid saponins, triterpenes, alkaloids, lignans, flavones, phytosterols, and volatile oils. Polysaccharides and steroid saponins are acknowledged as the principal pharmacologically active constituents of *P. sibiricum* extract. This study illustrates the effectiveness of alcohol extraction from *P. sibiricum* in suppressing the proliferation and migration of NSCLC both in vitro and in vivo, indicating promising anti-tumor properties. Differences in active ingredients resulting from diverse sources of the medicinal material can influence the effectiveness of drugs, underscoring the significance of evaluating the quality of herbal products utilized in studies. The intricate chemical composition of herbal products, characterized by numerous components present in minimal concentrations, requires the utilization of sophisticated analytical methods to ensure prompt and precise identification. In this study, UPLC-Q-TOF-MS/MS was utilized to examine the chemical components of alcohol extracts derived from *Polygonatum* rhizome. The steroidal saponins present in the *P. sibiricum* extract exhibit a propensity to produce $[M + HCOO]^-$ adduct ion peaks and $[M - H]^-$ excimer ion peaks when subjected to analysis in the low-level negative ion mode. MassLynx 4.1 software is employed for the identification of unidentified compounds. Within this software, the "ElementalComposition" calculation tool can be utilized to initially determine the

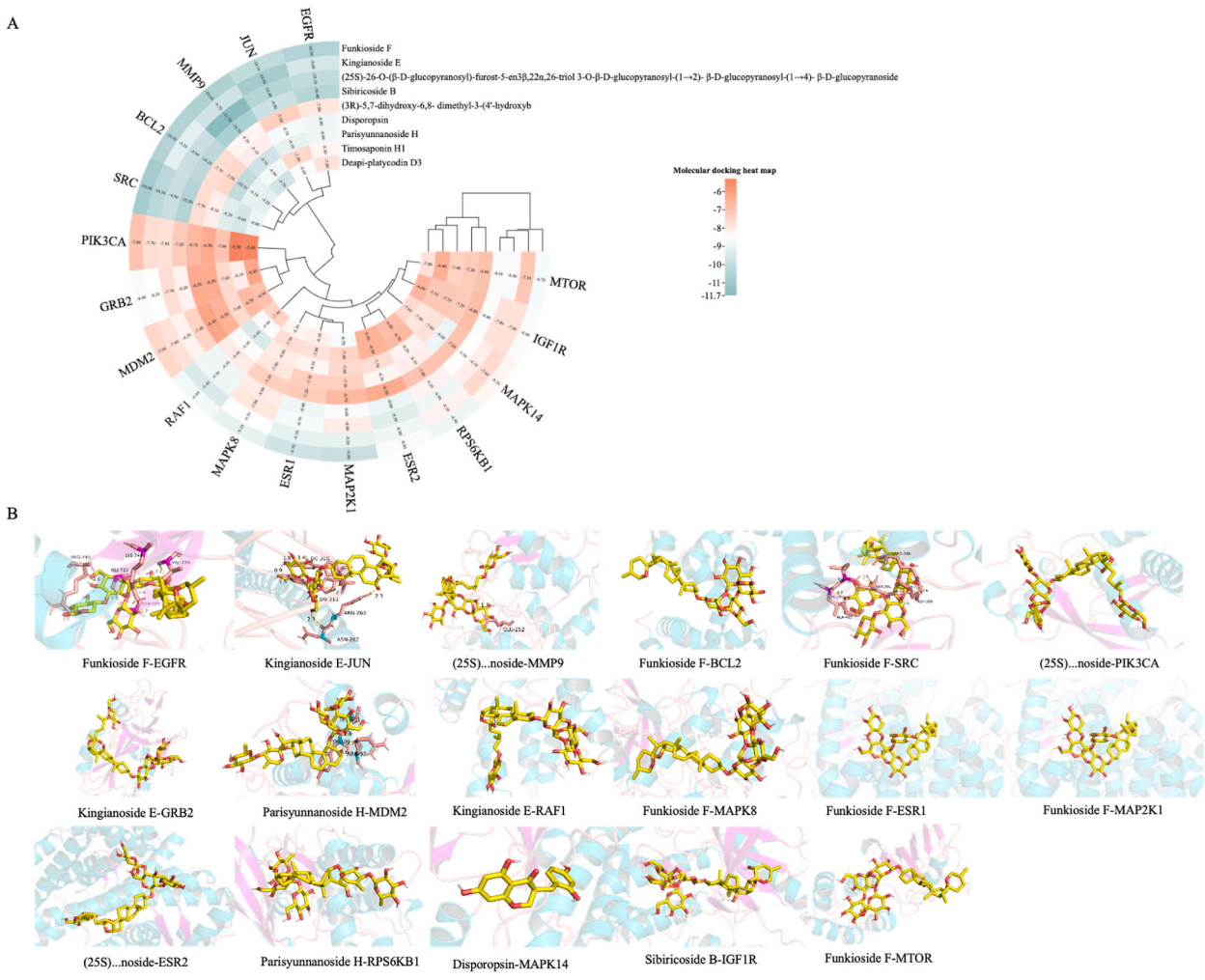

Fig. 10. Heatmap of molecular docking results (A) and pattern diagram (part) (B).

molecular formula of the compounds associated with individual chromatographic peaks. Through a comprehensive analysis involving the precise determination of relative molecular mass, retention time, fragmentation patterns observed in mass spectrometry, distinctive fragment ions, and relevant literature sources, a total of 17 chemical constituents present in the *P. sibiricum* extract were successfully identified. These constituents include twelve saponins, four flavonoids, and one amino acid. Currently, the majority of the literature available on these components is centered around *Polygonatum kingianum Coll. Et Hemsl.* and *Polygonatum sibiricum Red.*. Previous research has highlighted significant distinctions among *Polygonatum kingianum Coll. et Hemsl.*, *Polygonatum sibiricum Red.*, and *Polygonatum cyrtonema Hua.*, primarily attributed to the abundant presence of acetyl saponins in *Polygonatum sibiricum Red.* [32]. The outcomes of our analysis revealed the presence of acetyl groups in the saponins extracted from *P. sibiricum*. This finding offers a theoretical foundation for categorizing the resources of *P. sibiricum* and utilizing genuine medicinal materials in Shaanxi province. In this study, it was observed that all four flavonoids present in the *P. sibiricum* extract were identified as high isoflavones. High levels of isoflavones were identified as a characteristic component of the *P. sibiricum* genus. Flavonoids in *P. sibiricum* are primarily categorized into chalcone, dihydroflavonoid, and high isoflavone, with high isoflavone exhibiting the highest content. The parent nuclear structure of high isoflavone differs from isoflavones by only one additional carbon atom. Isoflavones are not naturally occurring compounds and are limited to a few plant species. Consequently, in the comprehensive qualitative and quantitative investigation of the characteristic components contributing to anti-tumor efficacy, certain steroids and flavonoids could serve as reliable indicators of the quality of *P. sibiricum*. Furthermore, certain components, particularly those exhibiting high response strength, remain unidentified due to constraints within the chemical composition database, necessitating further investigation.

In contrast to the research conducted by Huang et al. [42], which focused on the analysis and identification of components in 50% methanolic extracts of *P. sibiricum* flowers using UPLC-Q-TOF-MS/MS and identified a total of 64 compounds grouped into five distinct categories. Discrepancies were observed in both the chemical composition and the quantity of compounds identified in our investigation. Further investigation unveiled that the disparities originated from variations in the origin of the Chinese herbal medicine, the specific plant parts used for extraction, and the extraction solvent applied. *P. sibiricum* is a Chinese herbal medicine found in various

Table 4
Binding energy results(kcal/mol).

Targets	Compounds								
	(25S)-26-O-(β-D-glucopyranosyl)-furost-5-en3β,22α,26-triol3-O-β-D-glucopyranosyl-(1 → 2)-β-D-glucopyranosyl-(1 → 4)-β-D-glucopyranoside	Timosaponin H1	Deapi-platycodin D3	(3R)-5,7-dihydroxy-6,8-dimethyl-3-(4′-hydroxybenzyl)-chroman-4-one	Disporopsin	Funkioside F	Kingianoside E	Parisyunnanoside H	Sibiricoside B
BCL2	−9.9	−9.1	−9.2	−7.7	−7.5	−10.5	−9.2	−10.1	−10.2
EGFR	−10.1	−8.3	−7.8	−7.9	−8.9	−10.5	−9.6	−8.9	−10.4
ESR1	−8.7	−7.8	−8.1	−7.2	−7.3	−9.7	−9.1	−8.3	−8.9
ESR2	−9.3	−6.5	−6.5	−6.3	−8.3	−8.6	−8.9	−7.7	−9
GRB2	−7.7	−8.1	−6.2	−6.3	−6.3	−8.4	−8.5	−7.6	−8.2
IGF1R	−7.8	−7.1	−6.6	−6.8	−7.2	−8.6	−7.8	−7.1	−8.4
JUN	−10.4	−7.5	−8.6	−7.3	−8.7	−10.1	−10.9	−9.1	−9.8
MAP2K1	−8	−7.4	−8.7	−6.7	−7.3	−9.9	−9.1	−7.6	−8.6
MAPK14	−8.1	−7.9	−7.6	−7	−9	−8.3	−7.6	−7.8	−8.5
MAPK8	−7.9	−7.7	−8.3	−7.3	−7.9	−9.1	−8.5	−8	−8
MDM2	−8.2	−6.7	−6.9	−6.1	−6.5	−7.5	−7.8	−7.6	−7.4
MMP9	−11.7	−8.8	−9.7	−8.3	−8.1	−10.6	−9.7	−9.7	−10.7
mTOR	−8.4	−6.4	−7.8	−6.9	−7.2	−8.7	−7.1	−7.4	−8.6
PIK3CA	−7.8	−5.3	−5.4	−6.7	−6.3	−7	−7.7	−7	−7.2
RAF1	−8.9	−8.4	−7.4	−8	−8.4	−8.8	−9.4	−9.4	−8.9
RPS6KB1	−8.9	−6.7	−6.8	−7	−8.1	−8.9	−8.2	−8.2	−8.2
SRC	−9.9	−9.6	−9	−7.7	−8.1	−10.9	−10.3	−9.3	−10.5

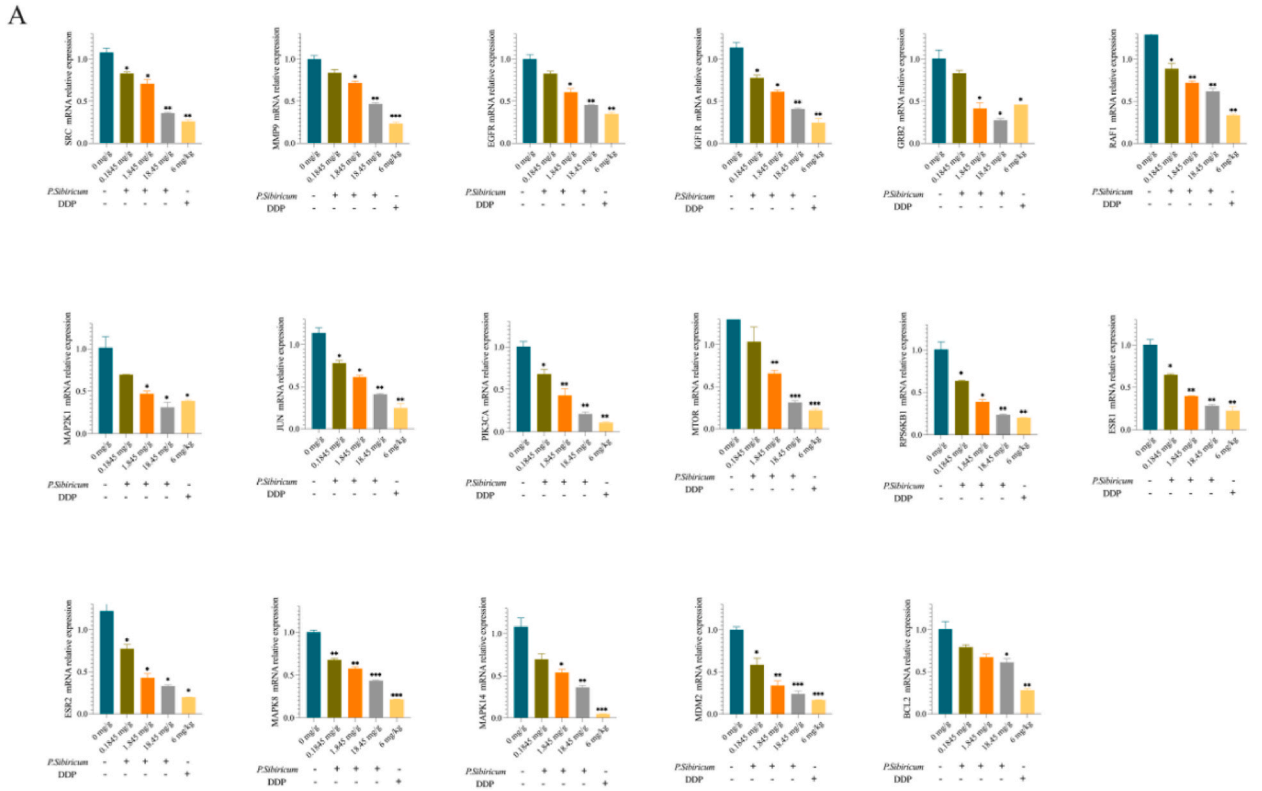

Fig. 11. The relative mRNA expression of key genes (BCL2, EGFR, ESR1, ESR2, GRB2, IGF1R, JUN, MAP2K1, MAPK14, MAPK8, MDM2, MMP9, mTOR, PIK3CA, RAF1, RPS6KB1 and SRC) in C57/BL6 transplanted tumor mice and NSCLC cells treated with *P. sibiricum* were detected by RT-qPCR. The C57/BL6 transplanted tumor model mice were given intragastric saline as model group, treated with *P. sibiricum* (0.1845, 1.845, and 18.45 mg/g) as *P. sibiricum* group, and treated with 6 mg/g DDP as positive control group. The cells incubated with cell culture-medium for 24 h as a blank control group and treated with *P. sibiricum* (3.39, 6.77, 13.54, 27.09, and 54.17 μg/mL) for 24 h as *P. sibiricum* group. (A) The mRNA expression of key genes in tumor-bearing mice. (B) The mRNA expression of key genes in NSCLC cell line H1299. (C) The mRNA expression of key genes in NSCLC cell line A549. Data are presented as the Mean ± SD (n = 3). (A) $^{*}P < 0.05$; $^{**}P < 0.01$ as compared with Model group. (B) (C)$^{*}P < 0.05$; $^{**}P < 0.01$ as compared with 0.00 μg/mL.

regions, including Shanhai Pass, Northern, Southern, Yun, and Gui herbal medicines. The quality of *P. sibiricum* varies depending on its origin. For instance, Yang et al. [40] analyzed the composition of *Polygonatum sibiricum Red.*, *Polygonatum cyrtonema Hua.*, and *Polygonatum kingianum Coll. et Hemsl.* from different production areas, highlighting significant variations in chemical constituents. Our study focused on analyzing the chemical constituents of *P. sibiricum* cultivated in Shaanxi Province, aiming to provide insights for quality control and resource development in this region. Another crucial factor that influenced the study outcomes was the specific plant parts that were examined. While our analysis focused on the rhizome of *P. sibiricum*, Huang et al. conducted research on the flower component. The last distinction lied in the choice of solvent utilized. In this investigation, ethanol was employed as the extraction solvent for the preparation of the test product solution. The consensus among researchers was that flavonoids were the primary components in *P. sibiricum* responsible for the treatment of tumors. Consequently, 50% ethanol was selected as the extraction solvent. The primary components extracted using ethanol were saponins and flavonoids, which corresponded with the findings of our analysis. In contrast, Huang et al. utilized a solvent extraction method with 50% methanol. While additional components have been identified, it remains unconfirmed whether the test product demonstrating anti-tumor activity in vivo or in vitro experiments. In contrast, we initially validated the notable anti-NSCLC efficacy of the 50% ethanol extracts of *P. sibiricum* through a combination of in vivo and in vitro experiments. Subsequently, the chemical components were identified using the UPLC-Q-TOF-MS. The analysis based on material properties rooted in pharmacodynamics has the potential to improve the development of *P. sibiricum* resources and provide a more reliable reference for the dual utilization in medicine and food.

Furthermore, network analysis tools were utilized to identify the primary targets of the *P. sibiricum* extraction. Through network pharmacology predictions and data analysis, 17 significant targets (BCL2, EGFR, ESR1, ESR2, GRB2, IGF1R, JUN, MAP2K1, MAPK14, MAPK8, MDM2, MMP9, mTOR, PIK3CA, RAF1, RPS6KB1, and SRC) associated with these components were anticipated. Subsequently, nine components, including (25S)-26-O-(β-D-glucopyranosyl)-furost-5-en3β,22α,26-triol3-O-β-D-glucopyranosyl-(1→2)-β-D-glucopyranosyl-(1→4)-β-D-glucopyranoside, Deapi-platycodin D3, (3R)-5,7-dihydroxy-6,8-dimethyl-3-(4′-hydroxybenzyl)-chroman-4-one, Timosaponin H1, Funkioside F, Kingianoside E, Disporopsin, Parisyunnanoside H, and Sibiricoside B, were found to closely bind to the

Fig. 11. (*continued*).

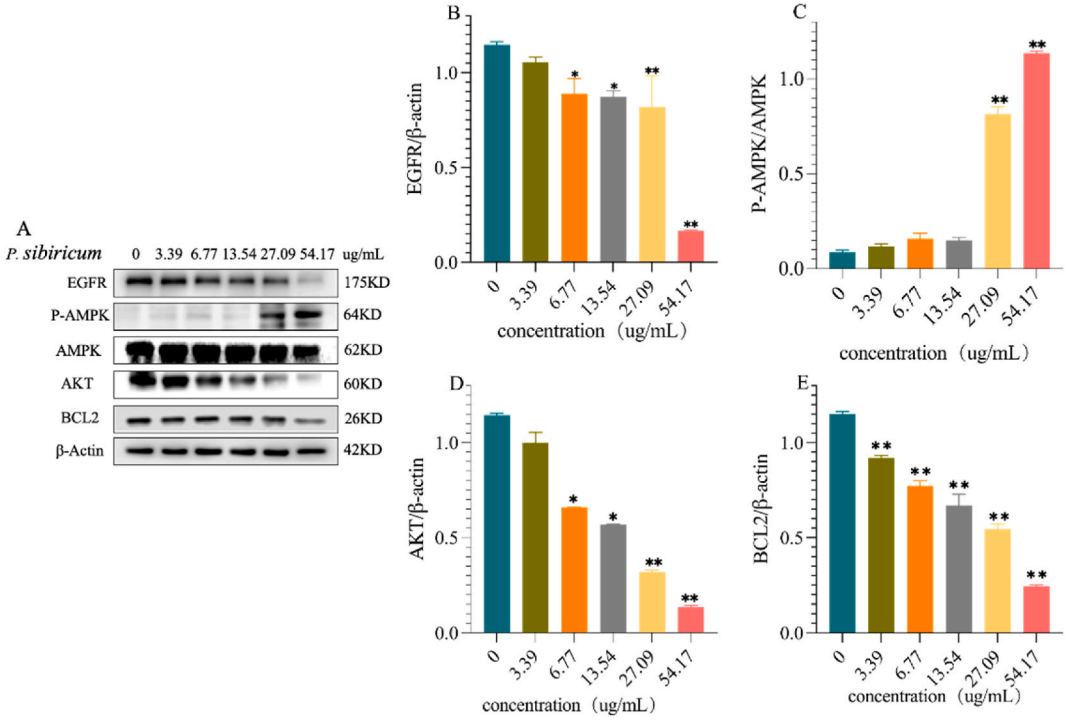

Fig. 12. Western blot analysis of NCI–H1299 cells treated with different doses of *P. sibiricum* for 24 h. (A) Expression of different proteins in NCI–H1299 cells. (B) Gray value of three parallel experiments of EGFR. (C) Gray value of three parallel experiments of P-AMPK. (D) Gray value of three parallel experiments of AKT. (E) Gray value of three parallel experiments of BCL2. Data are presented as the Mean ± SD (n = 3). $^{*}P < 0.05$; $^{**}P < 0.01$ as compared with 0.00 μg/mL.

core target through molecular docking. Among these, seven active ingredients were confirmed to be part of *P. sibiricum* saponins, while two active ingredients were identified as components of *P. sibiricum* flavonoids. Notably, (25S)-26-O-(β-D-glucopyranosyl)-furost-5-en3β,22α,26-triol3-O-β-D-glucopyranosyl-(1→2)-β-D-glucopyranosyl-(1→4)-β-D-glucopyranoside was identified as a steroid saponin. Although its anti-NSCLC effect remains unexplored, similar saponins have demonstrated inhibition of A549 proliferation with an IC50 of 38.6 μM [43]. Additionally, specific tumor-associated proteins such as MUC5B expression in lung adenocarcinomas have been suggested as potential biomarkers for adenocarcinomas. Deapi-platycodin D3 was found to significantly impact the production and secretion of airway mucin in both in vivo and in vitro models [44]. Timosaponin V, an analog of Timosaponin H1, exhibited notable cytotoxic activities against MCF-7 and HepG2 cell lines with IC50 values of 2.16 ± 0.19 μM and 2.01 ± 0.19 μM, respectively [45]. Furthermore, (3R)-5,7-dihydroxy-6,8-dimethyl-3-(4′-hydroxybenzyl)-chroman-4-one and disporopsin were qualitatively and quantitatively identified in *P. sibiricum* from various sources using chemical fingerprinting and chemometrics techniques [35]. 3-Benzylidene chroman-4-ones share close homology with naturally occurring bioactive compounds, these compounds exhibited anti-proliferative effects on breast cancer cell lines, increasing the sub-G0/G1 phase cell cycle and total apoptosis of MCF-7 cells. In addition, these compounds also showed excellent binding energy in the computational analysis of Akt enzyme binding [46]. While their role in NSCLC remains unexplored, AKT is closely associated with cell proliferation in various tumor types, suggesting that (3R)-5,7-dihydroxy-6,8-dimethyl-3-(4′-hydroxybenzyl)-chroman-4-one and disporopsin may inhibit NSCLC cell proliferation. The highest content of (25R)-Kingianoside E was observed among the 20 steroidal saponins identified in the extract of steroidal saponins from *Polygonatum cyrtonema Hua.* [47]. Parisrugosides H exhibited cytotoxicity against five human cancer cell lines, including human HL-60 leukemia, A549 lung, MCF-7 breast, SMMC-7721 liver, and SW480 colon solid cancer cell lines [48]. Consequently, this study provides initial evidence that the alcohol extract of *P. sibiricum* possesses a potent anti-NSCLC effect, with several chemical components showing current or potential anti-tumor effects. These findings underscore the necessity for further investigations into the relationship between specific compounds and targets.

An expanding body of evidence indicates that the therapeutic benefits of TCM are linked to its varied components and targets. This study utilizes network pharmacology as an innovative method for exploring drug therapies for various diseases. The analysis of core targets and pathway enrichment indicated that endocrine resistance, MAPK, and PI3K-AKT pathways could potentially serve as crucial factors in the treatment of NSCLC with *P. Sibiricum.* The network pharmacology analysis specifically emphasized the importance of the endocrine pathway, which includes 17 core targets (BCL2, EGFR, ESR1, ESR2, GRB2, IGF1R, JUN, MAP2K1, MAPK14, MAPK8, MDM2, MMP9, mTOR, PIK3CA, RAF1, RPS6KB1, and SRC), in influencing the treatment of NSCLC by *P. Sibiricum*. BCL2 protein which is highly expressed in NSCLC and associated with the development of NSCLC. Down-regulating BCL2 is beneficial to alleviate the clinical stage and node metastasis of NSCLC. The EGFR in the maintenance of epithelial tissue plays an important role. Over the past few decades,

EGFR targeted therapy has shaped a new era of precision oncology. EGFR mutation occurs in 10–15% of white and at least 30–50 % of Asia in patients with NSCLC, which were mostly initially sensitive to EGFR TKIs [49]. However, acquired resistance to EGFR TKI therapy inevitably emerges, and the 5-year survival rate of patients with EGFR-mutant metastatic lung adenocarcinoma treated with erlotinib or gefitinib is only 14.6 % [50]. Thus, the development of novel therapeutic strategies such as dual pathway inhibition have been found a promising strategy for patients with EGFR-Mutant NSCLC [51–54]. Growth factor receptor-binding protein 2 (GRB2) is an adaptor protein essential for phosphorylated residues of active EGFR a1nd their interaction is associated with active EGFR signaling and regulation of AKT/ERK/STAT3 signaling pathways [55]. Alpha lipoic acid and Lymecycline have been reported to be effective on inhibition the growth or reverses acquired EGFR-TKI resistance of NSCLC cells by targeting GRB2-mediated EGFR down-regulation [56,57]. Besides, it's more regrettable that some patients were primary resistance to EGFR-TKIs, MDM2 amplification may induce primary resistance to EGFR-TKIs and predict poor prognosis of NSCLC patients. Therefore, MDM2 may be a new biomarker and therapeutic target for NSCLC [58]. In this study, we could see *P. Sibiricum* were found has the characteristics of multiple targets, and it could down-regulated mRNA expression of both GRB2 and EGFR, and it could also be effect on down-regulate EGFR of EGFR insensitive cell line. MAPK14 inhibitors (trisubstituted imidazoles, SD-06, Amgen 16, RWJ67657 and SCIO-323) have been reported as the fourth-generation EGFR-TKIs to overcome the C797S resistance caused by L858R/T790 M/C797 EGFR mutant [59]. Survival analysis showed that the survival rate of the low expression group of ESR1 and MMP2 was higher than that of the high expression group, which further confirmed that reducing the expression of ESR1 and MMP2 could improve the quality of life of NSCLC patients [60]. A study related the prognostic biomarker for the patients with adjuvant chemotherapy after complete resection of early-stage NSCLC was carried by survival analysis and Cox hazards models through two independent datasets from GEO including a total of 309 patients, they made a conclusion that the low ESR2 expression in patients, the more survival benefit they had [61]. IGF1R plays a vital role in regulating a wide range of cellular processes, including proliferation, differentiation, survival and movement, and it also acts as a lung cancer metastasis-promoting factor [62,63]. IGF1R mRNA expression may be a prognostic biomarker in advanced NSCLC, a meta-analysis including 17 studies comprising 3294 patients drawn a conclusion that IGF1R positive expression was associated with an unfavorable DFS in NSCLC patients [64,65]. MAP2K1 mutations are rare in NSCLC and considered to be mutually exclusive from known driver mutations [66].The MAP2K1 K57 N mutation may still be associated with resistance in preclinical models, and potential targeting aberrations may often occur [67]. MAPK8 were reported exerting influence on the progression of several cancers, and play a vital role in NSCLC pathogenesis [68,69]. when MAPK8 was up-regulated, the lung aseno-carcinoma progression and the NSCLC cells invasion and migration would be promoted [70,71]. The matrix metalloproteinases (MMPs), a modulators of the tumor micro-environment, which represent the most prominent family of proteinases associated with tumorigenesis, and they can play roles in extracellular matrix transformation and cancer cell migration, regulating signaling pathways that control cell growth, inflammation, or angiogenesis, and may even act in a non-proteolytic manner [72]. Inhibiting MMPs like MMP2/9 could prevent metastasis of NSCLC [73,74]. On the contrary, high expression of MMPs will stimulate cancer invasion [75].The PI3K/Akt/mTOR pathway and signaling cascade is crucial in the regulation of cellular growth and metabolism. The presence of PIK3CA gene mutations or amplifications has been found in a diverse range of malignancies [76]. A number of specific inhibitors of PI3K (Alpelisib, GSK2636771, Taselisib, and SAR260301), Akt (Perifosine) and mTOR (Everolimus, Sirolimus, Temsirolimus, and Ridaforolimus) were currently under development and tried single or dural in various stages of preclinical investigation and in early phase clinical trials for NSCLC. The abnormal activation of RPS6KB1 predicts worse prognosis in NSCLC patients [77]. Raf1 is an independent novel prognostic factor and potential target for improving the long-time outcome of NSCLC patients [78]. The results of q PCR showed that *P. sibiricum* could significantly reduce the mRNA expression of those genes referred above, which was consistent with our prediction analysis, and *P. sibiricum* may inhibit NSCLC mainly through multi-targets.

In addition, JUN, MAPK8, MAPK14, GRB2, EGFR, MAP2K1, GF1R, RAF1and PRKCA were belong to the MAPK signaling pathway.

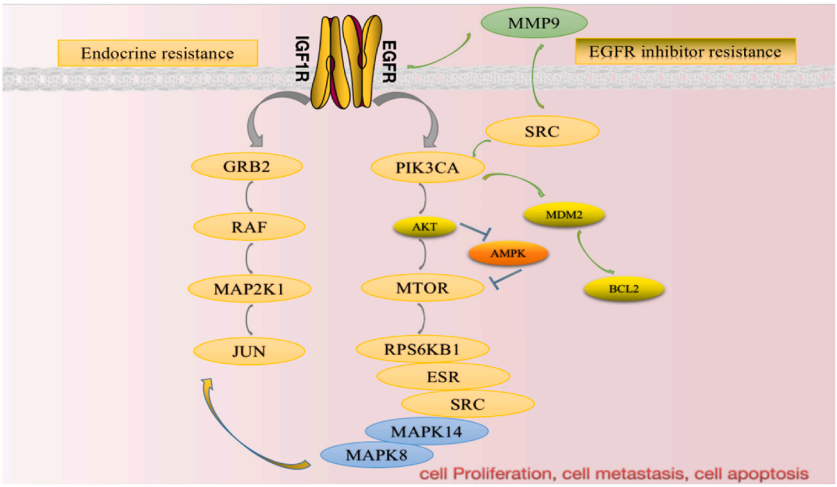

Fig. 13. The possible mechanism underlying *P. sibiricum* anti-cancer effect.

MAPK signal pathway, also known as mitogen-activated protein kinase signal pathway, is an important signal pathway involved in cell proliferation, differentiation, migration and apoptosis, they include extracellular signal-regulated kinase ERK1/2, Jun amino-terminal kinase (JNK), p38 protein and extracellular signal-regulated kinase 5 (ERK5) pathway. ERK-1/2, p38 and ERK5 pathways have definite regulatory effects on tumor cells. Study had shown that ERK1/2 and p-ERK1/2 were highly expressed in lung cancer tissues, which were closely related to tumor cell differentiation, clinical pathological stage and lymph node metastasis. EGFR is a cell surface receptor encoded by the HER1(ERBB1) gene, which belongs to the same tyrosine kinase family as Her2neu (Erbb2), Her3 (Erbb3) and HER4 (Erbb4). Its phosphorylation is related to various cell regulation, Inhibition of EGFR expression can be used to treat NSCLC by modulating the immune micro-environment. This is because EGFR can upregulate immune checkpoints such as PD-L1 and IDO1, making NSCLC more resistant to drugs [79]once it is over-expressed, the cell growth would be out of control, leading to malignant proliferation of tumor cells. These phosphorylated sites provide action sites for other downstream signaling molecules to promote tumor cell proliferation, differentiation, and migration by activating the downstream signaling pathways RAS-RAF-MEK-ERK and RAS-PI3k-PTEN-AKT-mTOR [80–85]. Fortunately, mTOR-induced cancer progression can be reversed by AMPK activation. KEGG enrichment analysis results have showed that these genes were most likely play roles through the endocrine resistance, MAPK and PI3K-AKT signalling pathway, which was consistent with our protein analysis results that different concentrations of *P. sibiricum* alcohol extraction could inhibit NSCLC proliferation through down-regulating EGFR and AKT, whereas activated p-AMPK and AMPK. And we can clearly see that a certain amount of *P. sibiricum* alcohol extraction could down-regulate the expression of BCL2 in NSCLC cell line H1299. Therefore, the *P. sibiricum* alcohol extraction has regulatory effect on MAPK signal transduction and interaction with PI3K-AKT and endocrine resistance. *P. sibiricum* could regulated cell proliferation, metastasis and apoptosis by many pathways (Fig. 13).

Endocrine therapy is essential in the comprehensive care of patients with hormone receptor-positive tumors, significantly improving patient prognosis. However, the issue of endocrine drug resistance presents a substantial barrier in the treatment of tumors. Extensive research in fundamental science has explored the mechanisms that underlie primary and acquired endocrine resistance. However, clinical efforts to combat endocrine drug resistance by targeting these mechanisms have generally yielded limited success. The resistance to endocrine therapy drugs is characterized by a multitude of mechanisms, which collectively diminish the effectiveness of drugs that target a single mechanism. Our study suggests that the application of *P. sibiricum* extract, which includes saponins, flavonoids, and other bioactive compounds, could potentially target multiple pathways to combat endocrine drug resistance. This presents a promising direction for future research in the field of tumor treatment.

Moreover, our inquiry uncovered inadequacies in certain index components present in the existing pharmacopoeia. The quality standard specified in the 2020 edition of the Chinese Pharmacopoeia focuses exclusively on the polysaccharide content, extract, and total ash content of *P. sibiricum*. While polysaccharides, reducing sugars, amino acids, 5-hydroxymethylfurfural, diosgenin, and 5-hydroxymethylmaltol have been identified by several sources as significant constituents of *P. sibiricum*, the establishment of precise regulatory thresholds lacks scientific substantiation. This study has provisionally recognized the pharmacodynamic elements accountable for the NSCLC properties of *P. sibiricum* as associated with its distinctive saponins and elevated isoflavones, thus providing a scientific basis for the identification of these pharmacodynamic components. Consequently, it is crucial to establish the acceptable content range by considering these fundamental ingredients.

In conclusion, this study confirmed the effectiveness of the ethanol extract obtained from *P. sibiricum* in suppressing the growth and movement of NSCLC cells through evaluations conducted both in laboratory settings and in living organisms. To set quality standards for the appropriate use of *P. sibiricum* extract in the treatment of NSCLC, the chemical components of the ethanol extract were identified using UPLC-Q-TOF-MS/MS for the first time. Moreover, the potential active components and molecular mechanisms of the ethanol extract from *P. sibiricum* against NSCLC were explored using network pharmacology. Through network predictions and subsequent in vitro and in vivo validations, it was hypothesized that *P. sibiricum* has the potential to induce apoptosis, inhibit proliferation and migration by modulating various components and targets within the endocrine resistance, MAPK, and PI3K-AKT pathways, thus demonstrating anti-NSCLC properties. However, there is a scarcity of research on the components of *P. sibiricum*. Therefore, additional experimental validation is required to clarify its fundamental material composition and molecular mechanisms.

Ethical approval

The animal experiments were approved by the Animal Experimental Ethics Committee of Shaanxi University of Traditional Chinese Medicine (SUCMDC20210310009).

Fundings

This study was supported by the National Natural Science Foundation of China (81402186); the Key Laboratory project of Shaanxi Provincial Department of Education (21JS015); and the Social Development Project of Department of Science and Technology of Shaanxi Province (2023-YBSF-294).

Data availability statement

All data generated or analyzed during this study are included in this published article. Raw data for this study are also available in the Supplemental Supporting Data Values file or from the corresponding author upon request.

CRediT authorship contribution statement

Kaili Guo: Writing – original draft, Validation, Software, Formal analysis, Data curation. **Yu Jiang:** Writing – original draft, Visualization, Validation, Formal analysis, Data curation. **Wei Qiao:** Writing – original draft, Visualization, Validation, Formal analysis, Data curation. **Panpan Yuan:** Validation, Software, Data curation. **Miao Xue:** Validation, Data curation. **Jiping Liu:** Conceptualization. **Hao Wei:** Conceptualization. **Bin Wang:** Conceptualization. **Xingmei Zhu:** Writing – review & editing, Supervision, Project administration, Investigation, Funding acquisition, Conceptualization.

Declaration of competing interest

The authors declare that they have no known competing financial interests or personal relationships that could have appeared to influence the work reported in this paper.

Appendix A. Supplementary data

Supplementary data to this article can be found online at https://doi.org/10.1016/j.heliyon.2024.e29166.

References

[1] A.L. Oliver, Lung cancer: epidemiology and screening, Surg. Clin. 102 (3) (2022) 335–344.
[2] R. Deshpand, M. Chandra, A. Rauthan, Evolving trends in lung cancer: epidemiology, diagnosis, and management, Indian J. Cancer 59 (Supplement) (2022) S90–S105.
[3] D.S. Ettinger, D.E. Wood, D.L. Aisner, et al., Non-small cell lung cancer, version 3.2022, NCCN clinical practice guidelines in oncology, J. Natl. Compr. Cancer Netw.: J. Natl. Compr. Cancer Netw. 20 (5) (2022) 497–530.
[4] Su X-E, Hong W-P, He H-F, et al. Recent advances in postoperative pulmonary rehabilitation of patients with non-small cell lung cancer (Review)[J]. International Journal of Oncology, 2022, 61(6): 156.
[5] R. Dziadziuszko, S. Peters, T. Ruf, et al., Clinical experience and management of adverse events in patients with advanced ALK-positive non-small-cell lung cancer receiving alectinib, ESMO open 7 (6) (2022) 100612.
[6] A. Zhang, F. Yang, L. Gao, et al., Research progress on radiotherapy combined with immunotherapy for associated pneumonitis during treatment of non-small cell lung cancer, Cancer Manag. Res. 14 (2022) 2469–2483.
[7] K. Long, K. Suresh, Pulmonary toxicity of systemic lung cancer therapy, Respirology 25 (Suppl 2) (2020) 72–79.
[8] Y.-P. Zhao, Y. Long, Pulmonary toxicity in driver gene positive non-small cell lung cancer therapy, Curr. Med. Res. Opin. 38 (8) (2022) 1369–1378.
[9] Z. Li, Z. Feiyue, L. Gaofeng, Traditional Chinese medicine and lung cancer–From theory to practice, Biomed. Pharmacother. 137 (2021) 111381.
[10] S. Wang, S. Long, Z. Deng, et al., Positive role of Chinese herbal medicine in cancer immune regulation, Am. J. Chin. Med. 48 (7) (2020) 1577–1592.
[11] L.-Q. Wan, Y. Tan, M. Jiang, et al., The prognostic impact of traditional Chinese medicine monomers on tumor-associated macrophages in non-small cell lung cancer, Chin. J. Nat. Med. 17 (10) (2019) 729–737.
[12] J. Yang, X. Zhu, P. Yuan, et al., Efficacy of traditional Chinese Medicine combined with chemotherapy in patients with non-small cell lung cancer (NSCLC): a meta-analysis of randomized clinical trials, Support. Care Cancer: Official Journal of the Multinational Association of Supportive Care in Cancer 28 (8) (2020) 3571–3579.
[13] X. Sui, M. Zhang, X. Han, et al., Combination of traditional Chinese medicine and epidermal growth factor receptor tyrosine kinase inhibitors in the treatment of non-small cell lung cancer: a systematic review and meta-analysis, Medicine 99 (32) (2020) e20683.
[14] Y. Shi, T.-G. Yang, M.-S. Yang, et al., [Polygonati Rhizoma: a crop with potential of being consumed as food and medicine], China J. Chin. Mater. Med. 47 (4) (2022) 1132–1135.
[15] Y. Hu, M. Yin, Y. Bai, et al., An evaluation of traits, nutritional, and medicinal component quality of polygonatum cyrtonema Hua and P. Sibiricum red, Front. Plant Sci. 13 (2022) 891775.
[16] J. Bi, C. Zhao, W. Jin, et al., Study on pharmacokinetics and tissue distribution of Polygonatum sibiricum polysaccharide in rats by fluorescence labeling, Int. J. Biol. Macromol. 215 (2022) 541–549.
[17] L.-H. Wu, G.-Y. Lv, B. Li, et al., [Study on effect of Polygonatum sibiricum on Yin deficiency model rats induced by long-term overload swimming], China J. Chin. Mater. Med. 39 (10) (2014) 1886–1891.
[18] F. Shen, Z. Song, P. Xie, et al., Polygonatum sibiricum polysaccharide prevents depression-like behaviors by reducing oxidative stress, inflammation, and cellular and synaptic damage, J. Ethnopharmacol. 275 (2021) 114164.
[19] C. Han, Y. Zhu, Z. Yang, et al., Protective effect of Polygonatum sibiricum against cadmium-induced testicular injury in mice through inhibiting oxidative stress and mitochondria-mediated apoptosis, J. Ethnopharmacol. 261 (2020) 113060.
[20] G. Ye, Y. Zhao, J. Zhu, et al., Synergistic effect of polydatin and polygonatum sibiricum polysaccharides in combating atherosclerosis via suppressing TLR4-mediated NF-κB activation in ApoE-deficient mice, Evid. base Compl. Alternative Med.: eCAM 2022 (2022) 3885153.
[21] H. Zhang, Y. Cao, L. Chen, et al., A polysaccharide from Polygonatum sibiricum attenuates amyloid-β-induced neurotoxicity in PC12 cells, Carbohydr. Polym. 117 (2015) 879–886.
[22] J. Su, Y. Wang, M. Yan, et al., The beneficial effects of Polygonatum sibiricum Red. superfine powder on metabolic hypertensive rats via gut-derived LPS/TLR4 pathway inhibition, Phytomedicine: International Journal of Phytotherapy and Phytopharmacology 106 (2022) 154404.
[23] P. Zhao, C. Zhao, X. Li, et al., The genus Polygonatum: a review of ethnopharmacology, phytochemistry and pharmacology, J. Ethnopharmacol. 214 (2018) 274–291.
[24] R. Hong-Min, D. Ya-Ling, Z. Jin-Lian, et al., [Research progress on processing history evolution, chemical components and pharmacological effects of Polygonati Rhizoma], China J. Chin. Mater. Med. 45 (17) (2020) 4163–4182.
[25] W. Zhou, J. Hong, T. Liu, et al., Polygonatum polysaccharide regulates macrophage polarization and improves LPS-induced acute lung injury through TLR4-MAPK/NF-κB pathway, Can. Respir. J. J. Can. Thorac. Soc. 2022 (2022) 2686992.
[26] X.-L. Li, X.-X. Zhang, R.-H. Ma, et al., Integrated miRNA and mRNA omics reveal dioscin suppresses migration and invasion via MEK/ERK and JNK signaling pathways in human endometrial carcinoma in vivo and in vitro, J. Ethnopharmacol. 303 (2023) 116027.
[27] X. Lu, Y. Zheng, F. Wen, et al., Study of the active ingredients and mechanism of Sparganii rhizoma in gastric cancer based on HPLC-Q-TOF-MS/MS and network pharmacology, Sci. Rep. 11 (1) (2021) 1905.
[28] M. Li, H. Luo, Z. Huang, et al., Screening and identification of anti-inflammatory compounds from erdong gao via multiple-target-cell extraction coupled with HPLC-Q-TOF-MS/MS and their structure-activity relationship, Molecules 28 (1) (2022) 295.

[29] R. Zhang, X. Zhu, H. Bai, et al., Network pharmacology databases for traditional Chinese medicine: review and assessment, Front. Pharmacol. 10 (2019) 123.
[30] B. Boezio, K. Audouze, P. Ducrot, et al., Network-based approaches in pharmacology, Molecular Informatics 36 (10) (2017).
[31] X. Wang, Z.-Y. Wang, J.-H. Zheng, et al., TCM network pharmacology: a new trend towards combining computational, experimental and clinical approaches, Chin. J. Nat. Med. 19 (1) (2021) 1–11.
[32] Y. Nan, Quality Analysis of Polygonati Rhizoma and Polygonati Rhizoma [D], Tianjin University of Traditional Chinese Medicine, 2022.
[33] L.-J. Guan, Study on the effective components of P.polyphylla var.chinensis and screening of key genes for the synthesis of steroidal saponins, D], Chinese Academy of Chinese Medical Sciences (2023).
[34] C.-Z. Wang, Study on Chemical Constituents and Antidepressant Effects of Different Parts of D.Kingianum [D], Jilin University, 2018.
[35] K. Zhou, M. Liu, J. Gao, et al., Discrimination of polygonati rhizoma species: an investigation utilizing high-performance liquid chromatography fingerprints and chemometrics, Chem. Biodivers. 20 (7) (2023) e202300458.
[36] Y. Gao, C.-L. Qi, L. Zhang, et al., Chemical constituents of fresh polygonati Rhizoma, Pharmaceutics and clinical research 23 (4) (2015) 365–367.
[37] H.-M. Ren, J.-L. Zhang, Y.-L. Deng, et al., UPLC-Q-TOF-MS-based chemical composition analysis of Polygonatum cyrtonema before and after processing, Chinese Journal of Experimental Prescriptions 27 (4) (2021) 110–121.
[38] Z.-H. Liang, Y.-J. Pan, L.-Y. Qiu, et al., UPLC-Q-TOF-MS/MS was used to analyze the changes of chemical components during the processing of Polygonati Rhizoma, Chinese herbal medicine 53 (16) (2022) 4948–4957.
[39] K.-Y. Ji, H.-P. Wang, J. Yang, et al., Rapid analysis and identification of chemical constituents of wild Polygonatum kingianum in Aba, Sichuan Province based on UPLC-Q-TOF-MS technology, Application Chemical Industry 48 (S1) (2019) 271–275.
[40] B. Yang, M. Golden, S.-J. Zheng, et al., UPLC-Q/TOF-MS-based component analysis of P. sibiricumm, P.cyrtonema and P.yunnanensis [J], J. Tradit. Chin. Med. 50 (10) (2022) 43–51.
[41] W. Zhou, J. Wang, Z. Wu, et al., Systems pharmacology exploration of botanic drug pairs reveals the mechanism for treating different diseases, Sci. Rep. 6 (2016) 36985.
[42] Z.-Z. Huang, X. Du, C. Ma, et al., Identification of antitumor active constituents in polygonatum sibiricum flower by UPLC-Q-TOF-MSE and network pharmacology, ACS Omega 5 (46) (2020) 29755–29764.
[43] G.A. Mohamed, S.R.M. Ibrahim, L.A. Shaala, et al., Urgineaglyceride A: a new monoacylglycerol from the Egyptian Drimia maritima bulbs, Nat. Prod. Res. 28 (19) (2014) 1583–1590.
[44] J. Ryu, H.J. Lee, S.H. Park, et al., Effects of the root of Platycodon grandiflorum on airway mucin hypersecretion in vivo and platycodin D(3) and deapi-platycodin on production and secretion of airway mucin in vitro, Phytomedicine: International Journal of Phytotherapy and Phytopharmacology 21 (4) (2014) 529–533.
[45] Y.-F. Zhao, J. Zhou, M.-J. Zhang, et al., Cytotoxic steroidal saponins from the rhizome of Anemarrhena asphodeloides, Steroids 155 (2020) 108557.
[46] G.S. Zaman, H. Kamli, S. Radhakrishnan, et al., Structure activity evaluation and computational analysis identify potent, novel 3-benzylidene chroman-4-one analogs with anti-fungal, anti-oxidant, and anti-cancer activities, Drug Dev. Ind. Pharm. 47 (9) (2021) 1459–1468.
[47] G. Liu, S. Feng, M. Sui, et al., Extraction and identification of steroidal saponins from Polygonatum cyrtonema Hua using natural deep eutectic solvent-synergistic quartz sand-assisted extraction method, J. Separ. Sci. 46 (7) (2023) e2200823.
[48] L.-L. Yu, S. Wang, J. Wang, et al., Steroidal saponin components and their cancer cell cytotoxicity from Paris rugosa, Phytochemistry 204 (2022) 113452.
[49] U. Batra, B. Biswas, K. Prabhash, et al., Differential clinicopathological features, treatments and outcomes in patients with Exon 19 deletion and Exon 21 L858R EGFR mutation-positive adenocarcinoma non-small-cell lung cancer, BMJ open respiratory research 10 (1) (2023) e001492.
[50] J.J. Lin, S. Cardarella, C.A. Lydon, et al., Five-year survival in EGFR-mutant metastatic lung adenocarcinoma treated with EGFR-TKIs, J. Thorac. Oncol.: Official Publication of the International Association for the Study of Lung Cancer 11 (4) (2016) 556–565.
[51] X. Le, M. Nilsson, J. Goldman, et al., Dual EGFR-VEGF pathway inhibition: a promising strategy for patients with EGFR-mutant NSCLC, J. Thorac. Oncol.: Official Publication of the International Association for the Study of Lung Cancer 16 (2) (2021) 205–215.
[52] N. Girard, New strategies and novel combinations in EGFR TKI-resistant non-small cell lung cancer, Curr. Treat. Options Oncol. 23 (11) (2022) 1626–1644.
[53] L. Paz-Ares, T.-E. Ciuleanu, M. Cobo, et al., First-line nivolumab plus ipilimumab combined with two cycles of chemotherapy in patients with non-small-cell lung cancer (CheckMate 9LA): an international, randomised, open-label, phase 3 trial, Lancet Oncol. 22 (2) (2021) 198–211.
[54] S. Gadgeel, D. Rodríguez-Abreu, G. Speranza, et al., Updated analysis from KEYNOTE-189: pembrolizumab or placebo plus pemetrexed and platinum for previously untreated metastatic nonsquamous non-small-cell lung cancer, J. Clin. Oncol.: Official Journal of the American Society of Clinical Oncology 38 (14) (2020) 1505–1517.
[55] M.I. Toki, D.E. Carvajal-Hausdorf, M. Altan, et al., EGFR-GRB2 protein colocalization is a prognostic factor unrelated to overall EGFR expression or EGFR mutation in lung adenocarcinoma, J. Thorac. Oncol.: Official Publication of the International Association for the Study of Lung Cancer 11 (11) (2016) 1901–1911.
[56] Y. Chen, J. Wu, H. Yan, et al., Lymecycline reverses acquired EGFR-TKI resistance in non-small-cell lung cancer by targeting GRB2, Pharmacol. Res. 159 (2020) 105007.
[57] L. Yang, Y. Wen, G. Lv, et al., α-Lipoic acid inhibits human lung cancer cell proliferation through Grb2-mediated EGFR downregulation, Biochem. Biophys. Res. Commun. 494 (1–2) (2017) 325–331.
[58] D. Sun, Y. Zhu, J. Zhu, et al., Primary resistance to first-generation EGFR-TKIs induced by MDM2 amplification in NSCLC, Mol. Med. 26 (1) (2020) 66.
[59] I. Ahmad, M. Shaikh, S. Surana, et al., p38α MAP kinase inhibitors to overcome EGFR tertiary C797S point mutation associated with osimertinib in non-small cell lung cancer (NSCLC): emergence of fourth-generation EGFR inhibitor, J. Biomol. Struct. Dynam. 40 (7) (2022) 3046–3059.
[60] Mingming Ma, Mingxin Zhang, The expression and significance of Rap1b in non-small cell lung cancer, Modern Oncology 23 (17) (2015) 2426–2428.
[61] H. Yu, D. Gu, P. Qian, Prognostic value of ESR2 expression on adjuvant chemotherapy in completely resected NSCLC, PLoS One 15 (12) (2020) e0243891.
[62] J. Shirakawa, T. Okuyama, E. Yoshida, et al., Effects of the antitumor drug OSI-906, a dual inhibitor of IGF-1 receptor and insulin receptor, on the glycemic control, β-cell functions, and β-cell proliferation in male mice, Endocrinology 155 (6) (2014) 2102–2111.
[63] E. Alfaro-Arnedo, I.P. López, S. Piñeiro-Hermida, et al., IGF1R acts as a cancer-promoting factor in the tumor microenvironment facilitating lung metastasis implantation and progression, Oncogene 41 (28) (2022) 3625–3639.
[64] A. Vilmar, E. Santoni-Rugiu, J.G.-F. Cillas, et al., Insulin-like growth factor receptor 1 mRNA expression as a prognostic marker in advanced non-small cell lung cancer, Anticancer Res. 34 (6) (2014) 2991–2996.
[65] S. Zhao, Z. Qiu, J. He, et al., Insulin-like growth factor receptor 1 (IGF1R) expression and survival in non-small cell lung cancer patients: a meta-analysis, Int. J. Clin. Exp. Pathol. 7 (10) (2014) 6694–6704.
[66] G. Harada, S.-R. Yang, E. Cocco, et al., Rare molecular subtypes of lung cancer, Nat. Rev. Clin. Oncol. 20 (4) (2023) 229–249.
[67] M. Scheffler, A. Holzem, A. Kron, et al., Co-occurrence of targetable mutations in Non-small cell lung cancer (NSCLC) patients harboring MAP2K1 mutations, Lung Cancer 144 (2020) 40–48.
[68] P. Xu, G. Zhang, S. Hou, et al., MAPK8 mediates resistance to temozolomide and apoptosis of glioblastoma cells through MAPK signaling pathway, Biomed. Pharmacother. 106 (2018) 1419–1427.
[69] W. Zhang, J. Sun, J. Luo, High expression of Rab-like 3 (Rabl3) is associated with poor survival of patients with non-small cell lung cancer via repression of MAPK8/9/10-mediated autophagy, Med. Sci. Mon. Int. Med. J. Exp. Clin. Res.: International Medical Journal of Experimental and Clinical Research 22 (2016) 1582–1588.
[70] W. Chen, G. Zheng, J. Huang, et al., CircMED13L_012 promotes lung adenocarcinoma progression by upregulation of MAPK8 mediated by miR-433-3p, Cancer Cell Int. 21 (1) (2021) 111.
[71] X. Zhang, G. Lei, K. Zhao, et al., CircTADA2A up-regulates MAPK8 by targeting MiR-214-3p and recruiting EIF4A3 to promote the invasion and migration of non-small cell lung cancer cells, Histol. Histopathol. 38 (7) (2023) 837–848.
[72] K. Kessenbrock, V. Plaks, Z. Werb, Matrix metalloproteinases: regulators of the tumor microenvironment, Cell 141 (1) (2010) 52–67.

[73] H. Jian, Y. Zhao, B. Liu, et al., SEMA4b inhibits MMP9 to prevent metastasis of non-small cell lung cancer, Tumour Biology: The Journal of the International Society for Oncodevelopmental Biology and Medicine 35 (11) (2014) 11051–11056.
[74] J. Li, H. Wang, H. Ke, et al., MiR-129 regulates MMP9 to control metastasis of non-small cell lung cancer, Tumour Biology: The Journal of the International Society for Oncodevelopmental Biology and Medicine 36 (8) (2015) 5785–5790.
[75] W. Zhang, T. Zhang, Y. Lou, et al., Placental growth factor promotes metastases of non-small cell lung cancer through MMP9, Cell. Physiol. Biochem.: International Journal of Experimental Cellular Physiology, Biochemistry, and Pharmacology 37 (3) (2015) 1210–1218.
[76] Y. Samuels, Z. Wang, A. Bardelli, et al., High frequency of mutations of the PIK3CA gene in human cancers, Science (New York, N.Y.) 304 (5670) (2004) 554.
[77] B. Chen, L. Yang, R. Zhang, et al., Hyperphosphorylation of RPS6KB1, rather than overexpression, predicts worse prognosis in non-small cell lung cancer patients, PLoS One 12 (8) (2017) e0182891.
[78] H. Tian, L. Yin, K. Ding, et al., Raf1 is a prognostic factor for progression in patients with non-small cell lung cancer after radiotherapy, Oncol. Rep. 39 (4) (2018) 1966–1974.
[79] B. Chen, Y. Song, Y. Zhan, et al., Fangchinoline inhibits non-small cell lung cancer metastasis by reversing epithelial-mesenchymal transition and suppressing the cytosolic ROS-related Akt-mTOR signaling pathway, Cancer Lett. 543 (2022) 215783.
[80] X.-L. Wang, X.-F. Jia, D.-Y. Tong, The drug resistance mechanism and countermeasures of non-small cell lung cancer after osimertinib treatment, Basic Clin. Oncol. 33 (4) (2020) 365–368.
[81] S.-J. Yue, P.-X. Zhang, Y. Zhu, et al., A ferulic acid derivative FXS-3 inhibits proliferation and metastasis of human lung cancer A549 cells via positive JNK signaling pathway and negative ERK/p38, AKT/mTOR and MEK/ERK signaling pathways, Molecules 24 (11) (2019) 2165.
[82] M.R. Zinatizadeh, S.R. Miri, P.K. Zarandi, et al., The hippo tumor suppressor pathway (YAP/TAZ/TEAD/MST/LATS) and EGFR-RAS-RAF-MEK in cancer metastasis, Genes & Diseases 8 (1) (2021) 48–60.
[83] V. Aran, J. Omerovic, Current approaches in NSCLC targeting K-RAS and EGFR, Int. J. Mol. Sci. 20 (22) (2019) 5701.
[84] W. Fang, Y. Huang, W. Gu, et al., PI3K-AKT-mTOR pathway alterations in advanced NSCLC patients after progression on EGFR-TKI and clinical response to EGFR-TKI plus everolimus combination therapy, Transl. Lung Cancer Res. 9 (4) (2020) 1258–1267.
[85] D. Zhang, L.-L. Han, F. Du, et al., FGFR1 induces acquired resistance against gefitinib by activating AKT/mTOR pathway in NSCLC, OncoTargets Ther. 12 (2019) 9809–9816.